

# 1 Rapidly Changing Lake-Terminating Glaciers in High 2 Mountain Asia: A Dataset from 1990 to 2022

3 Yunyi Luo<sup>1,2</sup>, Qiao Liu<sup>1</sup>, Xueyuan Lu<sup>1,2</sup>, Yongsheng Yin<sup>1,2</sup>, Jiawei Yang<sup>1,2</sup>, Xuyang  
4 Lu<sup>1</sup>

5 1 Institute of Mountain Hazards and Environment, Chinese Academy of Sciences, Chengdu 610041,  
6 China.

7 2 College of Resources and Environment, University of Chinese Academy of Sciences, Beijing 100049,  
8 China

9 Correspondence: Qiao Liu; liuqiao@imde.ac.cn

10 **Abstract.** Lake-terminating glaciers (LTGs) typically exhibit higher rates of retreat and thinning  
11 compared to land-terminating glaciers. However, a comprehensive inventory for LTGs and their  
12 associate proglacial lakes across High Mountain Asia (HMA) is currently lacking, limiting further  
13 understanding of their spatial heterogeneity in glacier change. This study employs a semi-automated  
14 identification method, coupled with rigorous visual inspection, to construct a comprehensive inventory  
15 of LTGs and proglacial lakes in HMA for 1990 and 2022. Our data indicate that, by 2022, HMA hosted  
16 1740 LTGs ( $5082.08 \pm 13.15 \text{ km}^2$ ), among which 667 glaciers ( $3454.59 \pm 12.43 \text{ km}^2$ ) remained in contact  
17 with proglacial lakes since 1990, 1073 ( $1627.49 \pm 4.30 \text{ km}^2$ ) are newly developed and 468 ( $960.13 \pm$   
18  $3.18 \text{ km}^2$ ) had disconnected from proglacial lakes during the investigation period. Accordingly, 645  
19 proglacial lakes ( $207.18 \pm 0.82 \text{ km}^2$ ) remained in contact with ice, 1123 new lakes ( $54.85 \pm 0.35 \text{ km}^2$ )  
20 formed, and 485 lakes ( $45.31 \pm 0.34 \text{ km}^2$ ) detached from ice (including 25 disappeared). During the past  
21 32 year, the total area of proglacial lakes increased by  $138.19 \pm 1.18 \text{ km}^2$  (81.7%), alongside a glacier  
22 area loss of  $324.43 \pm 19.23 \text{ km}^2$  (5.1%). The southern regions of HMA, particularly the Hindu Kush,  
23 Himalayas, Nyainqentanglha, and Gangdise Mountains, exhibiting the highest concentration and rapidest  
24 changes of the glacier-lake system. We hope that this dataset will improve our understanding of mountain  
25 glacier-lake interactions, water availability, as well as glacier-related hazards in HMA.

26 The dataset is [openly available in GeoPackage format, with full attribute tables compliant with the RGI](#)  
27 [7.0 vocabulary, and is hosted on Zenodo](#) at <https://doi.org/10.5281/zenodo.17369580> (Luo and Liu,  
28 2025).

设置了格式: 字体: Times New Roman

设置了格式: 字体: (默认) Times New Roman, 10 磅

设置了格式: 字体: 10 磅

29 **1 Introduction**

30 Proglacial lakes in direct contact with glacier termini play a critical role in glacier evolution (Liu et  
31 al., 2020; Truffer and Motyka, 2016; Chernos et al., 2016) and are a primary driver of spatial  
32 heterogeneity in glacier responses to climate change (Brun et al., 2019; Maurer et al., 2019). Proglacial  
33 lakes typically form behind end or lateral moraines, on debris-covered glaciers often developed through  
34 the coalescence of multiple supraglacial ponds near the glacier terminus (Carrivick and Tweed, 2013;  
35 Quincey et al., 2007; Mertes et al., 2017). The influence of lake water on glacier change operates  
36 primarily through two mechanisms: (1) thermal undercutting by lake water (Truffer and Motyka, 2016)  
37 and calving at the glacier front (Benn et al., 2007a), which together accelerate subaquatic and frontal  
38 ablation; and (2) when glacier termini come into contact with sufficiently deep water, the buoyancy of  
39 the lake reduces basal effective pressure, thereby enhancing glacier flow and dynamic thinning  
40 (Sugiyama et al., 2011; Sutherland et al., 2020; Benn et al., 2007b)(Sugiyama et al., 2011; Sutherland et  
41 al., 2020; Benn et al., 2007b), (Sato et al., 2022; Tsutaki et al., 2019; Tsutaki et al., 2017). Observations  
42 indicate that LTGs in High Mountain Asia (HMA) have mass loss rates 18–97% higher than the regional  
43 average (Brun et al., 2019) , and under comparable geographic conditions, their flow velocities are  
44 typically two- to threefold greater than those land-terminating counterparts (Pronk et al., 2021; Tsutaki  
45 et al., 2019). Furthermore, Zhang et al. (2023) reported that existing geodetic methods, by failing to  
46 account for the replacement of glacier ice by lake water, underestimate the mass loss of Himalayan LTGs  
47 by approximately 6.5%.

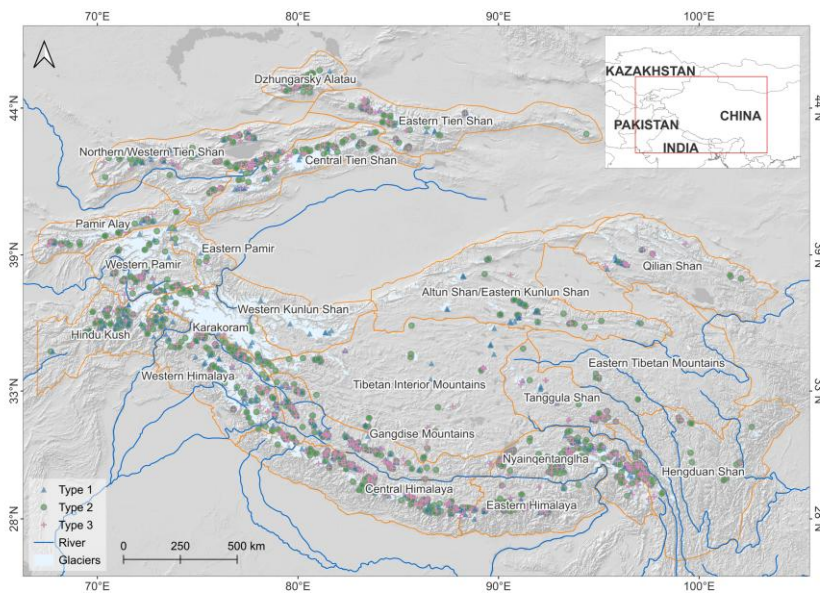
48 HMA encompassing the entire Tibetan Plateau and its surroundings contains the largest  
49 concentration of mid-latitude mountain glaciers on Earth. Driven by ongoing global warming, glaciers  
50 in HMA have undergone a persistent negative mass balance, with an average mass loss rate of  $-20.1 \text{ Gt}$   
51  $\text{a}^{-1}$  during 2000–2019 (Hugonnet et al., 2021). Glacier meltwater has driven substantial runoff and  
52 facilitated the formation and expansion of glacial lakes. From 1990 to 2018, the number of glacial lakes  
53 in HMA increased by 11%, and their total area expanded by 15% (Wang et al., 2020). The ongoing  
54 increase in both the number and extent of proglacial lakes underscores the critical need for a  
55 comprehensive assessment of lake-terminating glacier-proglacial lake systems in HMA. Such an  
56 evaluation is essential for elucidating feedback between the lake and ice, forecasting their responses to

域代码已更改

域代码已更改

57 future climate change, and informing evidence-based strategies for water resource management and  
 58 disaster risk mitigation. Although several regional-scale glacial lake inventories have been published in  
 59 recent years (Wang et al., 2020; Chen et al., 2021; Zhang et al., 2015; Worni et al., 2013; Salerno et al.,  
 60 2012; Shugar et al., 2020), most datasets do not distinguish the contact status and its change between  
 61 glaciers and proglacial lakes. Moreover, there is currently no comprehensive inventory of lake-  
 62 terminating glacier-proglacial lake systems covering the entire HMA, and their spatiotemporal evolution  
 63 remains poorly understood. Therefore, this study aims to construct a dataset of LTGs and proglacial lakes  
 64 for HMA based on multi-source remote sensing data, thereby filling this research gap and providing  
 65 fundamental database to support studies on regional glacier change, water resource assessment, disaster  
 66 management, and glacier hydrology.

## 67 2 Study area



68  
 69 **Figure 1.** Location of HMA and distribution of LTGs. Glacier outlines from the Randolph Glacier  
 70 Inventory (RGI v7.0). Types of LTGs are shown in Table 1.

71 High Mountain Asia (HMA), encompassing the Tibetan Plateau and its surrounding ranges-  
 72 including the Himalayas, Karakoram, and Pamir Plateau, etc.-constitutes the most glacier-rich region in

73 the mid-latitudes (Figure 1). HMA lies between 26°-45°N and 67°-105°E. It has an average elevation of  
74 approximately 4,500 m (SRTM DEM). The region features a complex topography. This topography is  
75 characterized by higher elevations in the northwest and lower elevations in the southeast. It comprises a  
76 network of interwoven mountain ranges, valleys, and river systems. The dominant orographic orientation  
77 is ~~east-west~~east-west. The Tanggula Shan, located in the central part of the region, rise above 6,000 m,  
78 while the Himalayas contain 15 peaks exceeding 8000 m, and most peaks on the northern plateau surpass  
79 6500 m. North-south trending ranges are mainly distributed in the southeastern Tibetan Plateau and the  
80 Hengduan Shan, forming the geomorphological framework of the region and controlling the overall  
81 topographic configuration of the plateau.

82 Climatically, ~~the southern part of HMA lies in the transition zone between~~is dominated by the South  
83 ~~Asian and East Asian monsoons, bringing abundant precipitation, whereas the northern and western~~  
84 ~~sectors are under the influence of the~~the mid-latitude westerlies and the Asian monsoon systems, leading  
85 ~~to pronounced seasonal and spatial contrast~~characterized by arid conditions and scarce precipitation  
86 (Yao et al., 2012). ~~In general, the southern and eastern sectors receive most precipitation during the~~  
87 ~~summer monsoon, whereas the northern and western sectors are more strongly influenced by the~~  
88 ~~westerlies, with overall drier conditions and a larger contribution from cold-season precipitation~~ (Khanal  
89 ~~et al., 2023).~~This pronounced hydroclimatic gradient produces north-south climatic contrast results in a  
90 highly heterogeneous ~~spatial~~ pattern of glacier accumulation and ablation across the region. HMA ~~is the~~  
91 ~~headwaters~~serves as the source region for several major Asian rivers, including the Yellow River, Yangtze  
92 River, Yarlung Tsangpo, Indus, Ganges, Salween, Mekong, and Irrawaddy, ~~which and thus plays an~~  
93 ~~important role in are vital for~~ downstream ~~hydrological-hydrology processes~~ and water resource  
94 ~~availability~~. According to the Randolph Glacier Inventory (RGI 7.0), HMA ~~hosts contain~~94,058,131,761  
95 modern glaciers ~~with a total area of, covering~~ approximately 99,468,462.7 km<sup>2</sup>, making it the most  
96 extensively glacierized region outside polar areas. ~~The Karakoram hosts the largest number of glaciers,~~  
97 ~~totaling 13,988, and also accounts for the largest share of glacier area at 29%. In contrast, the eastern~~  
98 ~~Tibetan Plateau contains the fewest glaciers, with 819. The Eastern Tibetan Mountains represent the~~  
99 ~~lowest glacier-area share, at 0.1%.~~ Most glaciers in HMA are undergoing retreat (Brun et al., 2017;  
100 Hugonnet et al., 2021). However, slight mass gains have been observed in parts of the Karakoram and

101 western Kunlun ranges (Gardelle et al., 2012; Kääb et al., 2015), though recent studies suggest this trend  
102 may be diminishing (Hugonnet et al., 2021). Glacial lakes are also widespread across HMA. Based on a  
103 recent manually interpreted inventory (Wang et al., 2020), 27205 and 30121 glacial lakes were mapped  
104 in 1990 and 2018, with total areas of 1806.47 ± 2.11 km<sup>2</sup> and 2080.12 ± 2.28 km<sup>2</sup>, respectively. This  
105 inventory includes the Altai and Sayan region, which is not part of our HMA definition. The largest lake  
106 areas were concentrated in the Altai and Sayan (335.42 ± 0.88 km<sup>2</sup>, 16.1% of the total) and the eastern  
107 Himalaya (310.37 ± 0.89 km<sup>2</sup>, 14.9%). In contrast, relatively small lake areas were found in the eastern  
108 Kunlun and Qilian Shan (38.85 ± 0.29 km<sup>2</sup>, 1.9%) and the eastern Tien Shan (40.55 ± 0.32 km<sup>2</sup>, 2.0%).  
109 Over 1990–2018, glacial lakes across HMA experienced widespread areal expansion, with an average  
110 increase of 15.2%

### 111 3 Data and methodology

#### 112 3.1 Extraction of proglacial lake outlines

113 Before developing a comprehensive inventory of LTGs shown in [Figure 1](#), we first generated a  
114 proglacial lake dataset using an automated delineation workflow within the Google Earth Engine (GEE)  
115 platform ([Figure 2](#)). We used Landsat imagery from the Thematic Mapper (TM) and Operational Land  
116 Imager (OLI) sensors, selected for their long-term record (since 1972), 30 m resolution, global coverage,  
117 and open access. All images were pre-processed in GEE, including radiometric, atmospheric, and  
118 geometric corrections. To minimize seasonal variability and the presence of snow and ice, we selected  
119 images acquired from July to November. Two-time windows were defined: 1990 ± 2 years (historical)  
120 and 2022 ± 1 year (recent). Due to limited image availability around 1990, imagery from 1993 to 1996  
121 was used to supplement data gaps. A 2 km buffer around each glacier was applied to focus on potential  
122 ice-contact proglacial lakes. Cloud contamination was reduced using the CFMask algorithm (Foga et al.,  
123 2017) to detect and mask clouds and shadows, followed by compositing cloud-free mosaics ([Figure 3a,](#)  
124 [b](#)). In total, 4570 Landsat TM scenes were used for the 1990 period and 5493 OLI scenes for the 2020  
125 period ([Figure 3e](#)[d](#), [d](#)).

设置了格式: 字体颜色: 自定义颜色( RGB(51,51,255) )

设置了格式: 字体颜色: 自定义颜色( RGB(51,51,255) )

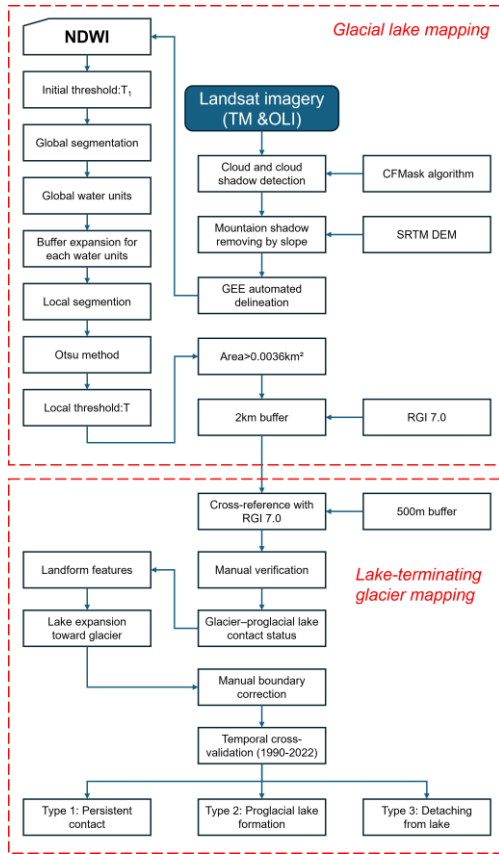


**Figure 2. Mapping workflow for lake-terminating glaciers and proglacial lakes**

Glacial lake extents were delineated using an automated mapping algorithm based on hierarchical image segmentation and terrain analysis (Li and Sheng, 2012; Zhang et al., 2017). To reduce the influence of mountain shadows, pixels with slopes  $>20^\circ$  or shaded relief values  $<0.25$  were excluded (Zheng et al., 2021b)(Zheng et al., 2021). Previous studies applied varying minimum area thresholds for glacial lake identification:  $0.0054 \text{ km}^2$  (Wang et al., 2020),  $0.0081 \text{ km}^2$  (Chen et al., 2021),  $0.0036 \text{ km}^2$  (Luo et al., 2020), and  $0.01 \text{ km}^2$  (Li et al., 2020). Smaller thresholds can lead to greater uncertainties due to the limitations of pixel resolution (Salerno et al., 2012). To improve the accuracy of lake-terminating glacier identification, we adopted a minimum lake area threshold of  $0.0036 \text{ km}^2$  (equivalent to at least four pixels), following Luo et al. (2020).

带格式的: 与下段同页

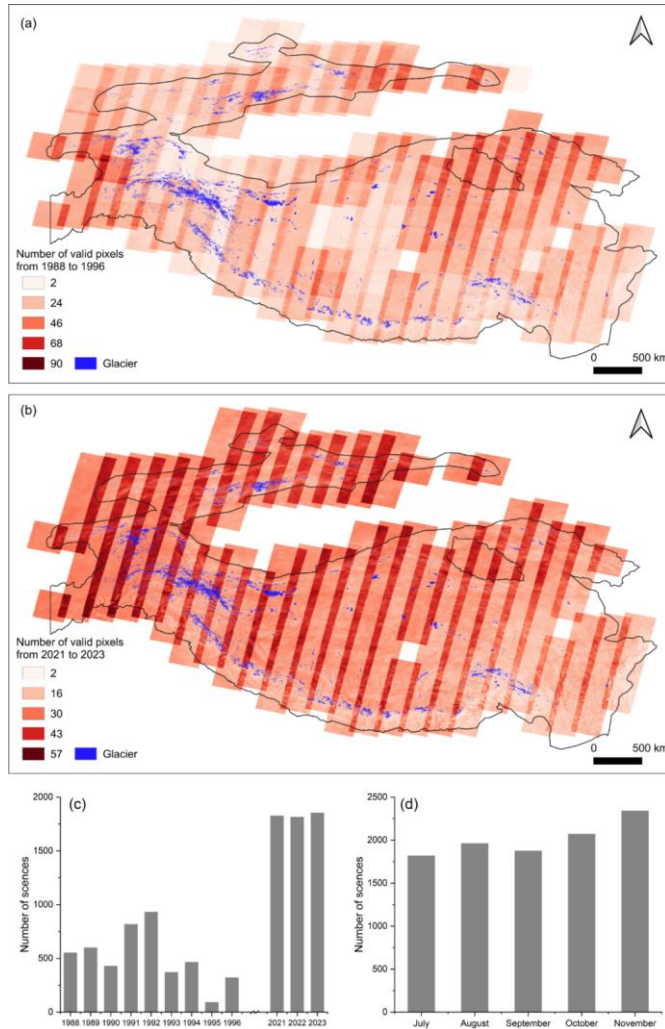
设置了格式: 字体: (默认) Times New Roman, 小五, 加粗

设置了格式: 字体: (默认) Times New Roman, 小五, 加粗

带格式的: 题注, 缩进: 首行缩进: 0 字符, 行距: 单倍行距

域代码已更改

域代码已更改



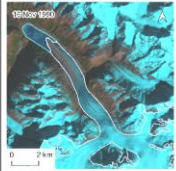
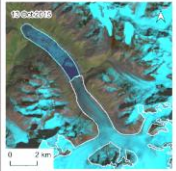
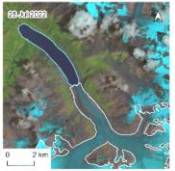
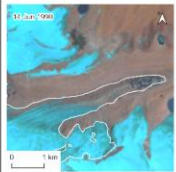
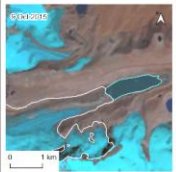
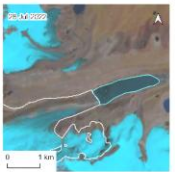
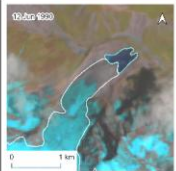
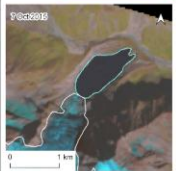
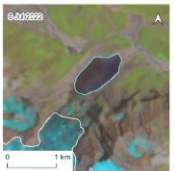
137  
 138 **Figure 3.** The number of usable pixels remaining in the study area after cloud removal during 1988–1996 (a)  
 139 and 2021–2023 (b). Temporal distribution of the number of images used, by year (c) and by month (d).

140 **3.2 Mapping of LTGs**

141 In this study, LTGs are defined as glaciers that develop proglacial lakes along the direction of ice  
 142 flow and are in direct contact with these lakes. The proglacial lake dataset was cross-referenced with the  
 143 RGI 7.0 glacier inventory to identify LTGs. Results were refined through detailed visual inspection and  
 144 manual correction using multi-source data, including Landsat and PlanetScopet-Labs imagery, online  
 145 maps (e.g., Google Earth, Esri basemap), and existing glacial lake datasets (Wang et al. 2020, Chen et al.

146 2021, Zhang et al. 2023). The identification of glacier-lake contact followed a two-step procedure. (1)  
147 Preliminary screening: A 500 m buffer was applied to assess spatial intersections between glacier  
148 boundaries and proglacial lakes, identifying potentially connected glacier-lake pairs. (2) Manual  
149 verification: Different criteria were applied for different periods. For the year 2020, multi-source  
150 moderate-to-high resolution imagery (e.g., Planet Labs, Landsat, Google Earth, Esri basemaps) was used.  
151 Glacier-lake contact was confirmed when proglacial lakes overlapped with glacier terminus and  
152 exhibited diagnostic geomorphic features, such as terminal ice cliffs or transverse crevasses  
153 perpendicular to the flow direction. Due to limited data availability and the relatively coarse spatial  
154 resolution of Landsat imagery (30 m) in 1990, direct identification of LTGs for that year involved  
155 considerable uncertainty, particularly for small glaciers, where boundary errors increase with decreasing  
156 glacier area. To address this, a temporal cross-validation approach was employed. Glaciers with  
157 ambiguous contact in 1990 were classified as interacting if satellite imagery from 1990 to 2022 showed  
158 lake expansion toward the glacier terminus. Based on the temporal evolution of glacier-lake contact,  
159 LTGs were categorized into three types (Table 1): (1) terminus persistent contacting with proglacial lake  
160 (Type 1); (2) terminus ~~expereneing~~ ~~experiencing~~ transition from supraglacial lake to proglacial lake (Type  
161 2); and (3) terminus detaching from proglacial lake (Type 3).

162 **Table 1.** The classification system of glaciers is based on the dynamic changes in glacier–lake contact. The  
 163 basemap is derived from Landsat imagery.

Types	Characteristics			
Type 1	Persistent contact between glacier and lake from 1990 to 2022.  Case location: 94.51053E, 30.63100N			
Type 2	Transition from supraglacial lake to proglacial lake from 1990 to 2022.  Case location: 88.23816E, 27.81772N			
Type 3	Detachment of the proglacial lake from the parent glacier from 1990 to 2022.  Case location: 85.84583E, 28.20793N			

164

### 165 3.3 Uncertainty estimates

166 When interpreting glacial lake and glacier boundaries using remote sensing data, errors are  
 167 inevitable even when manual visual delineation is applied. These errors are typically associated with  
 168 various factors related to image quality, such as spatial resolution, cloud cover, mountain shadows, and  
 169 subjective interpretation biases. Previous studies have reported that the area error in delineating glacier  
 170 or glacial lake boundaries from remote sensing imagery is approximately  $\pm 0.5$  pixels, depending on the  
 171 quality of the imagery. The uncertainty ( $\delta$ ) and relative error ( $E_l$ ) of glacial lake area was estimated using  
 172 the equation (Hanshaw and Bookhagen, 2014):

$$173 \quad \delta = \frac{P}{G} \times \frac{G^2}{2} \times 0.6872 \quad (3)$$

$$174 \quad E_l = \frac{\delta}{A} \times 100\% \quad (4)$$

175 where  $P$  is the perimeter of the glacial lake, and  $A$  is the glacial lake area.

176 The uncertainty ( $\lambda$ ) and relative error ( $E_g$ ) in glacier area was estimated to using the equation  
 177 (Bolch et al., 2010):

$$178 \quad \lambda = N \times \frac{G^2}{2} \quad (1)$$

9

179 
$$E_g = \frac{\lambda}{S} \times 100\% \quad (2)$$

180 where  $N$  is the total count of pixels along the outline of ice coverage,  $G$  is the spatial  
181 resolution of the images used, and  $S$  is the glacier area.

### 182 3.4 Attributes of inventory data

183 In this inventory, 9 attribute fields (Table 2) were recorded for the LTG, including a unique identifier,  
184 type, associated mountain range, area, mapping uncertainty, location (longitude and latitude), RGI7 ID,  
185 and feature code. Similarly, the proglacial lake inventory contains 9 attribute fields (Table 3), including  
186 a unique identifier, associated mountain range, type, mapping uncertainty, location (longitude and  
187 latitude), feature code, and a flag indicating whether the lake has disappeared. Both LTG and proglacial  
188 lake datasets include data for two time periods: 1990 and 2022, with identical attributes for both periods.  
189 The unique identifier is an automatically generated sequential integer, while the feature code follows the  
190 formats GmmmmmmEnnnnnN (Feature\_ID) for glaciers and GLmmmmmmEnnnnnN (Featue\_ID) for  
191 lakes, where G denotes glacier, GL denotes glacier lake, m and n represent the longitude and latitude  
192 multiplied by 1000, respectively, and E and N indicate east longitude and north latitude. Identical LTGs  
193 and proglacial lakes share the same feature code (Feature\_ID) to facilitate data linkage. Area and  
194 perimeter are calculated automatically from the feature geometry. The type of classification follows the  
195 criteria described in Section 3.2. Each feature's associated mountain range is determined by overlaying  
196 with mountain range boundaries, and mapping uncertainty is estimated according to Section 3.3.

197

198

199

200

201

202

203

204

205

206

207

208

**Table 2. Attributes of the glacier dataset**

Filed name	Type	Description
UID	Object ID	Unique code (Number)
Type	String	The classification of glaciers based on the relationship of interaction between glaciers and glacial lakes (Table 1)
Mountain	String	Mountain name where the glaciers is in
Area	Double	Area of glacier coverage(km <sup>2</sup> )
Error	Double	Area uncertainty of glacier mapping(km <sup>2</sup> )
Latitude	String	Latitude of the centroid of glacier
Longitude	String	Longitude of the centroid of glacier
rgi_id	String	RGI 7.0 id
Feature_ID	String	GmmmmmmEnnnnnN

209

210

**Table 3. Attributes of the proglacial lake dataset**

Filed name	Type	Description
UID	Object ID	Unique code (Number)
Type	String	The classification of glacial lakes based on the relationship of interaction between glaciers and glacial lakes (Table 1)
Mountain	String	Mountain name where the glacial lake is in
Area	Double	Area of glacial lake coverage (km <sup>2</sup> )
Error	Double	Area uncertainty of glacial lake mapping (km <sup>2</sup> )
Latitude	String	Latitude of the centroid of glacier
Longitude	String	Longitude of the centroid of glacier
Disappear	String	Whether the proglacial lake disappeared in 2022 (Y)
Feature_ID	String	GLmmmmmmEnnnnnN

211

## 212 4 Results

### 213 4.1 Spatial distribution of LTGs and proglacial lakes

214 Based on the changes in glacier-proglacial lake contact relationships from 1990 to 2022, glaciers  
215 were classified into three types (Table 1). Among them, Type 1 and Type 2 glaciers remained in contact  
216 with proglacial lakes from 1990 to 2022 and are therefore defined as LTGs. In contrast, Type 3 glaciers  
217 had become disconnected from proglacial lakes by 2022. Accordingly, only Type 1 and Type 2 glaciers  
218 were included when analyzing the distribution and extent of LTGs in 2022. In 2022, a total of 1740 LTGs  
219 were identified, with a combined area of  $5082.08 \pm 13.15 \text{ km}^2$ . Concurrently, 1768 proglacial lakes were  
220 detected, with a total area of  $262.10 \pm 0.89 \text{ km}^2$ . The discrepancy between glacier and lake counts stems  
221 from multi-lake associations per glacier and multi-glacier lakes were associated with two glaciers, and  
222 two lakes were in contact with three glaciers. The spatial distribution of LTGs in HMA shows marked  
223 heterogeneity (Figure 4). Predominantly concentrated along the southern margin, including the  
224 Himalayas, Nyainqentanglha, Gangdise Mountains, and Hindu Kush, these glaciers total 994,  
225 representing 57.13% of the study population (Figure 4b, Table S1). The Central Himalaya hosts the  
226 highest number, with 232 glaciers (), while the Nyainqentanglha accounts for the largest total glacier area  
227 ( $1,001.05 \pm 3.32 \text{ km}^2$ , Figure 4c). Glaciers were classified into nine size categories, ranging from  $<0.05$   
228  $\text{km}^2$  to  $>100 \text{ km}^2$  (Table A2S2). Among these, 1,095 glaciers (62.93%) are smaller than  $1 \text{ km}^2$ , covering  
229  $399.05 \pm 1.07 \text{ km}^2$  (7.85% of the total area), while 93 glaciers (5.35%) exceed  $10 \text{ km}^2$ , covering  
230  $2964.68 \pm 4.85 \text{ km}^2$  (58.34%). Only three glaciers exceed  $100 \text{ km}^2$ , spanning  $785.42 \pm 10.96 \text{ km}^2$ . LTGs in HMA  
231 span elevations from 2,735 to 8,016 m, with a mean elevation of 5074 m (Figure 5). They are primarily  
232 concentrated between 5,000 and 6,000 m, where their combined area reaches  $3030.2 \pm 5.72 \text{ km}^2$  (59.52%  
233 of the total glacier area). Regional variations in elevation distribution are evident (Figure 5). In the  
234 Central Himalaya, Eastern Himalaya, Gangdise Mountains, Tibetan Interior Mountains, and Western  
235 Kunlun Shan, glacier area peaks occur around 6000 meters.

236 Proglacial lakes in HMA are predominantly concentrated along the southern margin, with 1010  
237 lakes (57.09%) in the Himalayas, Nyainqentanglha, Gangdise Mountains, and Hindu Kush (Table S3).  
238 The Central Himalayas host the most lakes (240), with the largest total area ( $86.91 \pm 0.54 \text{ km}^2$ , Figure 4  
239 e). Proglacial lakes were grouped into five size categories ( $<0.05$  to  $>1 \text{ km}^2$ , Table S4). Lakes smaller

240 than 0.1 km<sup>2</sup> are the most abundant, totaling 1384 (78.28%) and covering a combined area of 47.12 ±  
241 0.30 km<sup>2</sup>. Proglacial lakes in HMA span elevations from 2684 to 6012 m, with most concentrated  
242 between 5000 and 5700 m, where 748 lakes (42.34%) cover 106.46 ± 0.59 km<sup>2</sup>. Regional variations in  
243 elevation distribution are evident (Figure 6). Gangdise Mountains and Western Kunlun Shan, proglacial  
244 lake numbers and areas peak around 5700 m. Conversely, in the Hindu Kush, Nyainqentanglha, Tanggula  
245 Shan, and Western Kunlun Shan, peak lake areas occur at lower elevations than peak lake numbers  
246 (Figure 6).

247 Significant variations exist in the number and area distributions among glacier types in HMA. From  
248 1990 to 2022, Type 2 glaciers, those forming new proglacial lakes, were the most numerous (1073, Table  
249 S1), dominating in all regions except Altun Shan/Eastern Kunlun Shan, Qilian Shan, and Tanggula Shan.  
250 Conversely, Type 1 glaciers have the largest total area (3454.59 ± 12.43 km<sup>2</sup>), concentrated primarily  
251 in the Himalayas, Nyainqentanglha, Central Tien Shan, Qilian Shan, Tanggula Shan, and Western Kunlun  
252 Shan (Table S1). The Central Himalaya host the most glaciers across all types: 94 Type 1 (552.77 ± 2.71  
253 km<sup>2</sup>), 138 Type 2 (244.80 ± 1.56 km<sup>2</sup>), and 84 Type 3 (202.67 ± 1.11 km<sup>2</sup>). All glacier types show  
254 consistent area peaks between 5,000 and 6,000 m, with similar patterns across subregions (Figure 5). In  
255 2022, Type 2 proglacial lakes were the most numerous in HMA (1123, Table S3Table A3), dominating  
256 in number across all regions except Altun Shan/Eastern Kunlun Shan, Qilian Shan, Karakoram, and  
257 Western Kunlun Shan. Conversely, Type 1 lakes had the largest total area (207.18 ± 0.82 km<sup>2</sup>) and  
258 accounted for the largest share of total area in all regions except the Western Pamir, Hengduan Shan,  
259 Dzhungarsky Alatau, and Eastern Tibetan Mountains. The central Himalaya hosted the greatest  
260 abundance of all three lake types, with 91 Type 1 (76.89 ± 0.51 km<sup>2</sup>), 149 Type 2, and 80 Type 3 (15.70  
261 ± 0.21 km<sup>2</sup>) lakes. The Eastern Himalaya had the largest Type 2 lake area (10.73 ± 0.03 km<sup>2</sup>, Table  
262 S3Table A3). In HMA, the elevation distribution of proglacial lake types is generally consistent, with  
263 peak numbers between 5000 and 5700 m and peak areas between 4700 and 5400 m (Figure 6). However,  
264 regional variations are observed in the elevation distribution of lake numbers for different lake types.  
265 Specifically, in the Nyainqentanglha region, Type 2 proglacial lakes exhibit a higher peak number range,  
266 between 5200 and 5400 m. Regarding area-elevation patterns, certain subregions display lower peak

267 elevations, encompassing Type 2 lakes in the Eastern Himalaya and Northern Tibetan Mountains, and  
268 Type 1 lakes in the Eastern Pamirs, Hindu Kush, Nyainqentanglha, and Tanggula Shan (Figure 5).

#### 269 4.2 Temporal changes in LTGs and proglacial lakes

270 From 1990 to 2022, glacier size has been continuously shrinking (Figure 4d). The total  
271 area of all glacier types decreased by approximately  $324.43 \pm 19.22 \text{ km}^2$ , with Type 1 glaciers  
272 experiencing the largest absolute loss of  $137.46 \pm 17.62 \text{ km}^2$ , accounting for 42.37% of the total  
273 reduction (Table S5). The Central Himalaya showed the most pronounced absolute area loss, with  
274 a decrease of  $74.46 \pm 3.46 \text{ km}^2$ , while the Hengduan Shan exhibited the highest relative  
275 shrinkage at 16.42%. The Central Himalaya also recorded the largest absolute losses for all  
276 three glacier types, with reductions of  $37.20 \pm 3.91 \text{ km}^2$  for Type 1,  $20.13 \pm 2.26 \text{ km}^2$  for Type  
277 2, and  $17.13 \pm 1.62 \text{ km}^2$  for Type 3 glaciers. In contrast, the Hengduan Shan had the highest  
278 relative losses for all three types, at 25.34%, 13.95%, and 17.37%, respectively (Table S5).

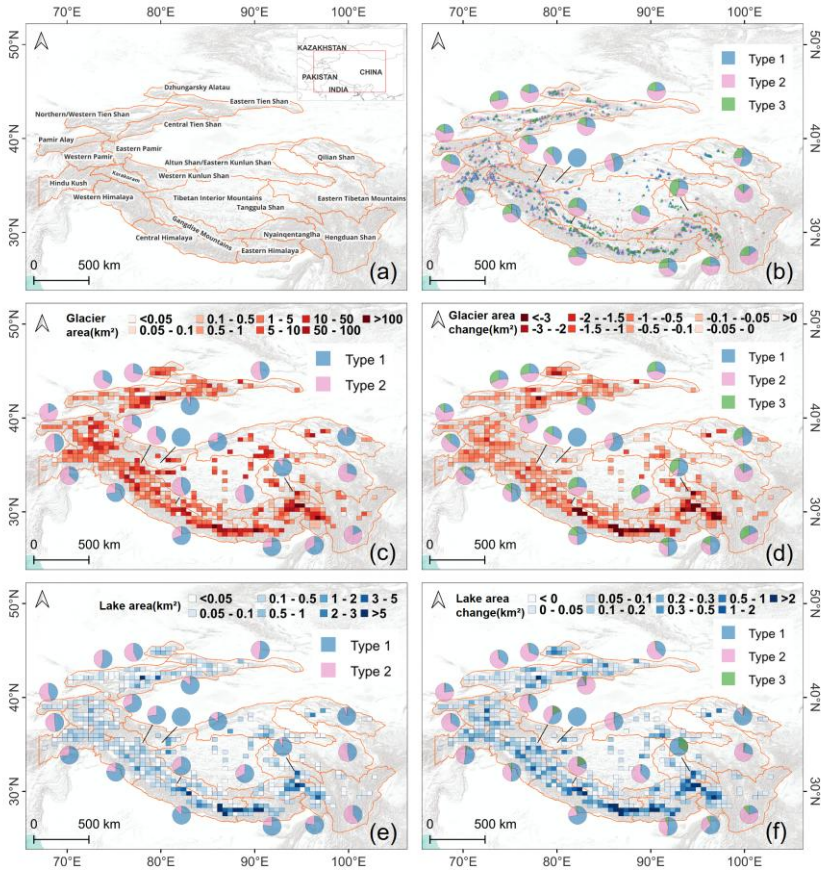
279 Small glaciers ( $<0.5 \text{ km}^2$ ) exhibited a significant increase in number, particularly those  
280 smaller than  $0.05 \text{ km}^2$ , which grew by 51 in count with a total area increase of  $1.68 \pm 0.08 \text{ km}^2$   
281 (Table S6). In contrast, glaciers in the  $0.5\text{--}50 \text{ km}^2$  range showed a declining trend in number.  
282 Among them, glaciers sized  $0.5\text{--}1 \text{ km}^2$  experienced the largest numerical decrease ( $-57$ ) and  
283 the greatest relative area loss ( $-13.56\%$ ), while those in the  $1\text{--}5 \text{ km}^2$  range incurred the most  
284 substantial absolute area reduction, losing  $97.17 \pm 3.5 \text{ km}^2$  (Table S6).

285 Among the different glacier types, Type 1 glaciers experienced the greatest absolute area  
286 loss, decreasing by  $137.46 \pm 17.62 \text{ km}^2$  (Table S5). However, their relative area reduction of  
287 3.83% was the smallest among the three types. By size class (Table S6), Type 1 glaciers showed  
288 the largest loss ( $63.39 \pm 6.38 \text{ km}^2$ ) in the  $10\text{--}50 \text{ km}^2$  range; Type 2 glaciers experienced the  
289 greatest reduction ( $52.52 \pm 2.21 \text{ km}^2$ ) in the  $1\text{--}5 \text{ km}^2$  range. Type 3 glaciers showed the most  
290 significant loss ( $27.51 \pm 1.57 \text{ km}^2$ ) in the  $5\text{--}10 \text{ km}^2$  range. For all three types, the  $0.5\text{--}1 \text{ km}^2$   
291 size class exhibited the highest relative area reduction, at 9.06%, 15.37%, and 15.15%,  
292 respectively.

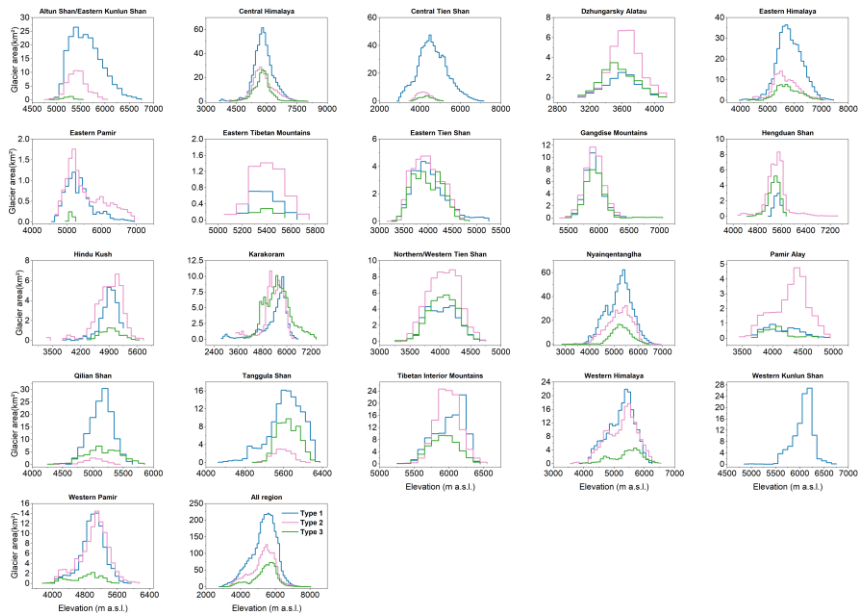
293 Between 1990 and 2022, the total area of proglacial lakes increased by  $138.19 \pm 1.18 \text{ km}^2$ ,  
294 representing a 62.09% expansion (Figure 4f and Table S2-Table A2). The Central Himalaya

295 experienced the most significant absolute growth, with an increase of  $42.32 \pm 0.72 \text{ km}^2$   
296 (70.19%), while the Western Pamirs recorded the fastest relative growth, surging by 210.24%.  
297 The Central Himalaya also saw the largest area increases across all three glacier types, with  
298 growth of  $30.42 \pm 0.64 \text{ km}^2$  for Type 1 lakes,  $10.02 \pm 0.16 \text{ km}^2$  for Type 2, and  $1.88 \pm 0.29 \text{ km}^2$   
299 for Type 3. Regionally, the Dzhungarsky Alatau had the highest proportional increase in Type  
300 1 lake area at 176.38%, whereas the Eastern Himalaya recorded the largest proportional growth  
301 for Type 3 lakes at 29.48% (Table S7-Table A7).

302 During the study period, 1123 new proglacial lakes formed, while 25 lakes disappeared.  
303 The number of small proglacial lakes ( $<0.5 \text{ km}^2$ ) increased significantly, especially those  
304 smaller than  $0.05 \text{ km}^2$ , which increased by 702 and accounted for 64.11% of the total increase  
305 in lake numbers (Table S8). Lakes larger than  $1 \text{ km}^2$  contributed the largest increase in area  
306 ( $60.44 \pm 0.81 \text{ km}^2$ ), accounting for 43.74% of the total area growth. Moreover, lakes smaller  
307 than  $0.05 \text{ km}^2$  had the highest proportional area growth at 114.49%. Type 1 proglacial lakes  
308 exhibited the most significant area growth, reaching  $79.36 \pm 1.02 \text{ km}^2$ , with a growth rate of  
309 62.09%. Among size categories, the number of Type 1 lakes increased most in the  $0.05\text{--}0.1 \text{ km}^2$   
310 range, with 49 new lakes added, while lakes larger than  $1 \text{ km}^2$  showed the greatest area  
311 increase at  $52.07 \pm 0.79 \text{ km}^2$  and the highest proportional growth at 85.19%.



312  
 313 **Figure 4.** (a) Geographic extent of the mountain ranges in HMA. (b) Distribution of the three types of LTGs  
 314 in 2022 and their numerical proportions across mountain regions. (c) Size distribution (Types 1 and 2) in 2022  
 315 and their area proportions. (d) Area changes of the three types of glaciers from 1990 to 2022 and their area-  
 316 change proportions across mountain regions. (e) Area distribution of proglacial lakes (associated with Types  
 317 1 and 2 glaciers) in 2022 and their area proportions across mountain regions. (f) Area changes of the three  
 318 types of proglacial lakes from 1990 to 2022 and their area-change proportions across mountain regions.  
 319

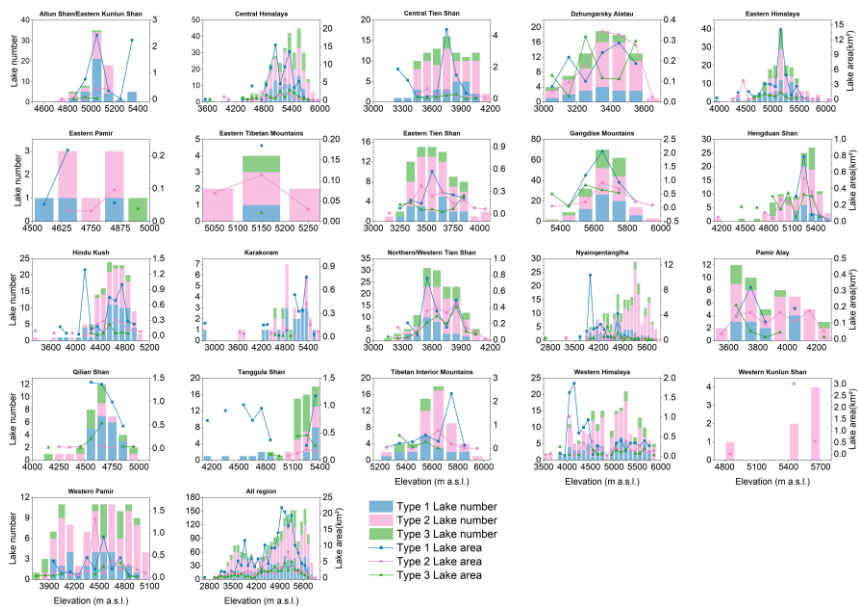


320

321

322

**Figure 5.** Area-Elevation distribution of LTGs across subregions, showing glacier area within 100 m elevation bins.



323

324

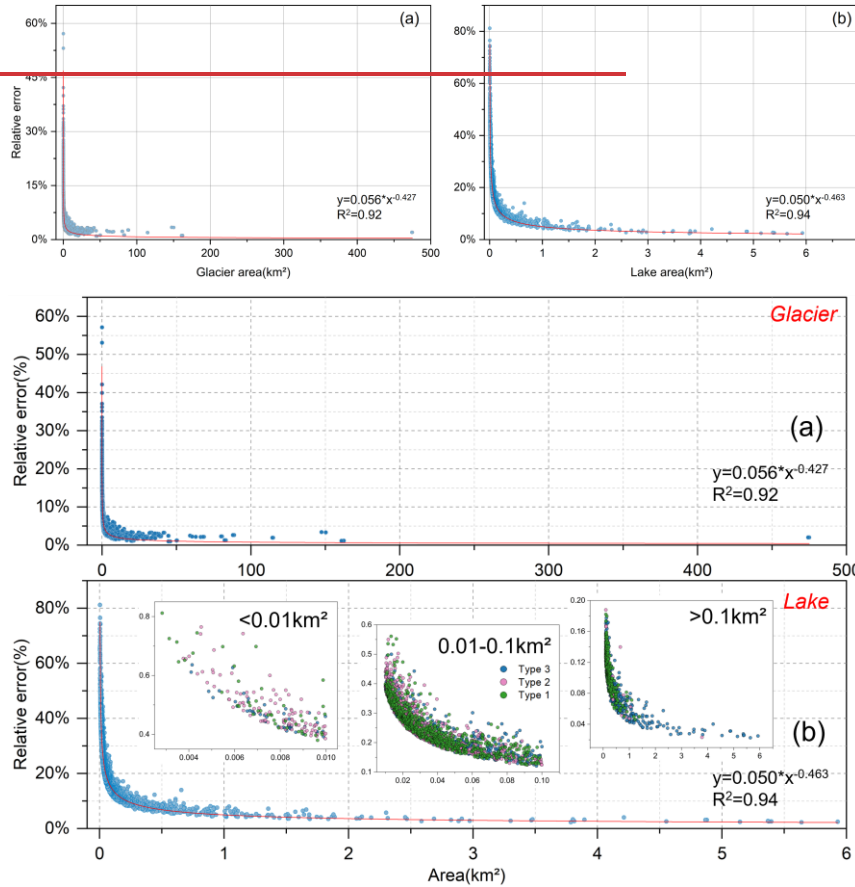
325

**Figure 6.** Distribution of proglacial lake numbers and areas across elevation ranges in each subregion. The number and area of proglacial lakes are presented within 100 m elevation bins for each subregion.

326 **5 Discussion**

327 **5.1 Assessment of accuracy and errors**

328 The uncertainty estimates indicate that as the glacier or lake area increases, the relative error of  
329 individual features decreases. In the study area, the total absolute area error for glaciers in 1990 and 2022  
330 were  $\pm 13.65 \text{ km}^2$  and  $\pm 13.53 \text{ km}^2$ , respectively, with average relative errors of  $\pm 7.24\%$  and  $\pm 8.12\%$ .  
331 The relative error of glacier area shows a significant power-law relationship with the glacier size ( $y =$   
332  $0.056 \times x^{-0.427}$ ,  $R^2 = 0.92$ , [Figure 7a](#)). Additionally, the total absolute area error for proglacial lakes  
333 in 1990 and 2022 were  $\pm 0.69 \text{ km}^2$  and  $\pm 0.96 \text{ km}^2$ , respectively, with average relative errors of  $\pm 21.99\%$   
334 and  $\pm 23.69\%$ , following a similar significant power-law relationship ( $y = 0.050 \times x^{-0.463}$ ,  $R^2 = 0.94$ ,  
335 [Figure 7b](#)). We found that the maximum relative error for proglacial lakes exceeds 80%. We therefore  
336 stratified relative error statistics by lake area bins and glacier types. The largest errors are primarily  
337 associated with lakes smaller than  $0.01 \text{ km}^2$ , which have a mean relative error of 49%. Within this size  
338 class, Type 2 proglacial lakes are most prevalent, accounting for 52% of all lakes  $< 0.01 \text{ km}^2$ . To better  
339 constrain the impact of these small lakes on overall dataset accuracy, we visually verified them using  
340 higher resolution remote sensing imagery (PlanetScope, Esri basemaps, and Google imagery), thereby  
341 reducing misidentification arising from limited spatial resolution.



342

343

344 **Figure 7.** Estimation of relative errors for glaciers and proglacial lakes in the study area. (a) Glaciers (b)  
 345 **Proglacial lakes.** We also divided the proglacial lakes into three area intervals and quantified the relative  
 346 **errors for different types.**

347 **5.2 Comparison and limitations**

348 Publicly available data on LTGs and their proglacial lakes in HMA remain scarce, with recent  
 349 datasets primarily focusing on glacial lakes. Consequently, this study selected two glacial lake datasets  
 350 that partially overlap in time with our research and include proglacial lakes for comparison (Table 4).  
 351 The results indicate that, within the same study area, our data closely align with those of Zhang et al.  
 352 (2023). In 1990, the overlap rate of proglacial lakes between the dataset of Zhang et al. (2023) and ours  
 353 exceeded 90%, while in 2020/2022, the overlap rate was 79%. In contrast, significant discrepancies were  
 354 observed with the dataset of Chen et al. (2021). For the period 2017/2022, the dataset of Chen et al. (2021)

设置了格式: 字体颜色: 自定义颜色( RGB(51,51,255) )

355 identified 7850 proglacial lakes, whereas our study identified only 1,768, with an overlap rate of 67.82%.  
356 To further clarify the causes of these discrepancies, we selected a representative subregion in the central  
357 Himalaya as a sample area for cross-validation (Fig. S1). Our dataset indicates that 45 proglacial lakes  
358 were present in this area in 2022. In contrast, Chen et al. (2021) reported 335 glacial lakes in 2017, of  
359 which only 29 (64% of our proglacial lakes) overlap with our inventory. Zhang et al. (2023) reported 38  
360 proglacial lakes in 2020, with 30 (67%) overlapping with our results. Chen et al. (2021) likely used a  
361 more permissive definition when screening lakes in front of glacier termini, effectively including many  
362 water bodies that are not in direct contact with glacier. We apply strict criterion (Sect. 3.2) and define  
363 proglacial lakes as those that are in contact with glacier ice and situated at the downstream end along the  
364 glacier flow direction. Part of the mismatch may also arise from differences in lake-type labeling during  
365 transitional stages. Several water bodies that we classify as proglacial lakes were labeled as supraglacial  
366 lakes by Chen et al. (2021) and Zhang et al. (2023). In addition, some supraglacial ponds are currently  
367 merging and evolving into a single, unified proglacial lake, and we classify lakes with a high degree of  
368 transition as proglacial lakes. Differences in the minimum mapping area threshold further amplify the  
369 mismatch. Our inventory and Zhang et al. (2023) uses 0.0036 km<sup>2</sup>, whereas Chen et al. (2021) used  
370 0.0081 km<sup>2</sup>, which affects the inclusion of small lakes and therefore the total lake count. Finally, we  
371 corrected omissions in earlier inventories where applicable, and Through examining these datasets, we  
372 attribute these differences to variations in the identification of glacier-proglacial lake contact. Our study  
373 employs strict classification criteria (see Section 3.2), which are reflected in three key aspects: (1) the  
374 lake must be located at the forefront of the glacier's flow direction; (2) a comprehensive evaluation of  
375 the glacier lake contact surface based on the spatiotemporal evolution of both lake and glacier surface  
376 morphology; and (3) exclusion of ambiguous cases to ensure classification reliability. Additional factors,  
377 such as image quality, acquisition dates, and vectorization workflows, may also contribute to the  
378 observed discrepancies.

379 A global inventory of LTGs was released in 2025 (Steiner et al., 2025). This dataset was derived  
380 from the RGI7 glacier outlines, primarily using Landsat 5–7 TM/ETM+ imagery (ca. 1998–2002),  
381 supplemented by ASTER data in some high-latitude regions (for a small portion of the Canadian Arctic  
382 and Greenland Periphery). Existing regional proglacial lake inventories (when close to 2000) were also

383 incorporated, and the identification of LTGs was conducted through manual interpretation and expert  
384 cross-validation. Based on the degree of glacier–lake contact, glaciers were classified into ~~four~~ three  
385 types (Level 1: glacier–lake contact exceeds 50% of the terminus perimeter. Level 2 : glacier–lake contact  
386 ranges from 10% to 50% of the terminus perimeter. Level 3: glacier–lake contact is less than 10% of the  
387 terminus perimeter.). In HMA, a total of 1912 LTGs were identified. Although the glacier termini in this  
388 dataset were delineated for  $2000 \pm 2$ , the overlap with our 2022 dataset is ~~47-45~~ 50%. Specifically, our  
389 dataset shows an overlap rate of 63% with level 1 glaciers, 43% with level 2 glaciers, and 19% with level  
390 3 glaciers. The differences in results can be attributed to two primary factors. First, temporal differences.  
391 The reference dataset is mainly based on imagery from around the year 2000, whereas our dataset relies  
392 on imagery from around 2022. Given that glacier–lake contact relationships are inherently unstable (Luo  
393 et al., 2025), the emergence of newly formed proglacial lakes and glaciers that no longer maintain contact  
394 with proglacial lakes during this period may have significantly influenced the statistical outcomes.  
395 Second, methodological differences. Although both studies adopt a broadly similar semi-automatic  
396 approach to screening glaciers based on lake data, the specific implementations differ. The reference  
397 dataset utilizes existing open-access lake inventories (Chen et al., 2021; Wang et al., 2020), while our  
398 lake dataset was extracted by ourself, with different lake area thresholds applied (0.0054 km<sup>2</sup> and 0.0081  
399 km<sup>2</sup> in the reference dataset versus 0.0036 km<sup>2</sup> in our study). Such differences may contribute to  
400 discrepancies in the results. Moreover, the criteria for identifying lake-terminating glaciers also diverge.  
401 The reference dataset classifies glaciers according to the proportion of lake contact relative to the glacier  
402 terminus perimeter, whereas our study emphasizes geomorphological features (e.g., ice cliffs, crevasses)  
403 and the expansion trend of proglacial lakes, i.e., whether lakes continue to expand toward the glacier.  
404 Due to these differences in classification standards, our dataset may not include some of the level 2 and  
405 level 3 glaciers identified in the reference dataset, which likely explains the lower overlap rates with  
406 these categories.

407 ~~–Given that our results indicate that glacier–lake contact is not always stable, differences in the~~  
408 ~~timing of terminus delineation are likely the primary source of the observed discrepancies.~~

409 Although this study employed standardized criteria for the qualitative identification of LTGs and  
410 their proglacial lakes, subjective factors remain challenging to eliminate entirely during remote sensing

411 imagery analysis. Differences in how analysts interpret imagery, apply calibration standards, and process  
 412 data quality directly impact the results. While measures such as independent labeling and cross-validation  
 413 by multiple analysts can reduce subjective bias, uncertainties stemming from variations in individual  
 414 experience, judgment criteria, and image quality remain difficult to fully resolve. Consequently, further  
 415 quantification of identification criteria is of paramount importance. In the future, more refined technical  
 416 approaches can optimize the identification of glacier-lake contact lines, leveraging high-resolution  
 417 imagery and automated analysis tools to enhance accuracy. Additionally, quantifying the depth of glaciers  
 418 within lakes will provide more precise data support. These quantitative standards not only effectively  
 419 minimize human-induced variability but also significantly improve the precision of glacier-lake contact  
 420 relationship assessments, laying a more reliable data foundation for subsequent studies of glacier  
 421 dynamics.

422 **Table 4. Comparisons of glacial lake mapping in this study with previous studies for the similar extended**  
 423 **region.**

Year (previous/this study)	Region	Area threshold (km <sup>2</sup> )	Source	Count (Area/km <sup>2</sup> )	Count (Area/km <sup>2</sup> )	Overlap count
				Previous studies	This study	
1990/1990	Greater Himalaya	0.0036	(Zhang et al., 2023)	651(129.76±0.89)	645(122.08±0.59)	615(95.35%)
2020/2022				1115(192.42±1.23)	1029 (199.83±0.79)	841(79.11%)
2017/2022	HMA	0.0081	(Chen et al., 2021)	7850(684.62±10.06)	1768(262.03±0.89)	1199(67.82%)

424 **5.3 Drivers of changes in lake-terminating glaciers and associated disaster risks**

425 Climate warming is a primary driver of both the number and size of proglacial lakes, which in turn  
 426 has contributed to the increasing prevalence of lake-terminating glaciers (LTGs). Glaciers across High  
 427 Mountain Asia (HMA) have experienced widespread retreat during the 21st century (Brun et al., 2017;  
 428 Hugonnet et al., 2021), with the most significant mass losses occurring in the Nyainqentanglha region  
 429 ( $-0.62 \pm 0.23$  m w.e. a<sup>-1</sup>, locally reaching  $-0.80 \pm 0.25$  m w.e. a<sup>-1</sup>). Moderate mass losses are observed  
 430 in the central Himalaya, with rates of  $-0.42 \pm 0.20$  m w.e. a<sup>-1</sup> in Bhutan and  $-0.33 \pm 0.20$  m w.e. a<sup>-1</sup> in  
 431 eastern Nepal. Consequently, the Himalayan-southeastern Tibetan Plateau has emerged as a hotspot of  
 432 glacier wastage. Glacier retreat provides both the material supply and geomorphic setting for proglacial

- 设置了格式: 字体: (默认) Times New Roman, (中文) 宋体, 10 磅, 加粗, 字体颜色: 自动设置
- 带格式的: 标题 2
- 带格式的: 缩进: 首行缩进: 2 字符, 行距: 1.5 倍行距
- 设置了格式: 字体: (默认) Times New Roman, 10 磅
- 设置了格式: 字体: (默认) Times New Roman, 10 磅
- 设置了格式: 字体: (默认) Times New Roman, 10 磅
- 设置了格式: 字体: (默认) Times New Roman, 10 磅
- 设置了格式: 字体: (默认) Times New Roman, (中文) + 中文正文 (等线), 10 磅
- 设置了格式: 字体: (默认) Times New Roman, 10 磅
- 设置了格式: 字体: (默认) Times New Roman, 10 磅
- 设置了格式: 字体: (默认) Times New Roman, (中文) + 中文正文 (等线), 10 磅
- 设置了格式: 字体: (默认) Times New Roman, 10 磅
- 设置了格式: 字体: (默认) Times New Roman, (中文) + 中文正文 (等线), 10 磅
- 设置了格式: 字体: (默认) Times New Roman, 10 磅
- 设置了格式: 字体: (默认) Times New Roman, (中文) + 中文正文 (等线), 10 磅
- 设置了格式: 字体: (默认) Times New Roman, 10 磅

433 lake development, fostering a high concentration of LTGs in this region. LTGs in the Himalayan–  
434 southeastern Tibetan Plateau account for 61% of the total number of LTGs in HMA and 55% of newly  
435 formed LTGs.

436 However, the formation of proglacial lakes is not solely driven by climate forcing; it also amplifies  
437 the nonlinear response of glaciers to climate change. Proglacial lakes are closely linked to enhanced  
438 glacier mass loss, primarily through processes such as subaqueous melting (Zhang et al., 2023),  
439 accelerated ice flow (Prong et al., 2021), and the potential risk of glacial lake outburst floods (Zheng et  
440 al., 2021b). As glacial lakes expand, the increasing water depth at glacier termini further elevates the  
441 uncertainty surrounding calving, as greater water depths are generally thought to accelerate terminus  
442 collapse (Minowa et al., 2023). Incorporating glacier morphological variables (e.g., supraglacial debris  
443 cover, slope, elevation) into the analysis is, therefore, essential for understanding the role of proglacial  
444 lakes in influencing glacier mass balance. Monitoring of Bridge Glacier by Chernos et al. (2016) revealed  
445 that calving at the glacier terminus has consistently remained a secondary contributor to ablation. While  
446 calving accounted for up to 49% of ablation in some individual years, its multi-year average contribution  
447 was only 10–25%. Rapid retreat has been strongly associated with increasing water depth, but such high  
448 calving rates are typically transient and tend to decrease as glacier termini recede into shallower waters.  
449 Our results further demonstrate that glacier-lake contact relationships are inherently unstable. Between  
450 1990 and 2022, 41% of glaciers that were previously in contact with proglacial lakes lost this connection.  
451 This rapid change underscores the episodic and unstable nature of the influence of proglacial lakes on  
452 glacier evolution. Therefore, projections of glacier mass loss should consider not only climatic factors  
453 but also the evolving glacier-lake contact relationships and their heterogeneous impacts on glacier  
454 dynamics.

455 The risk of glacial lake outburst floods (GLOFs) in the High Mountain Asia (HMA) region is  
456 increasing under the backdrop of climate warming, particularly in the Himalaya (Zheng et al., 2021b).  
457 Our study finds that the total area of proglacial lake expansion in the southeastern Tibetan Plateau and  
458 eastern Himalayas accounts for 78% of the total glacial lake expansion in the HMA. As glaciers retreat,  
459 proglacial lakes in contact with them expose their basins. This significantly increases their potential for  
460 expansion compared to other types of glacial lakes, making them a higher-risk disaster source. Over the

带格式的: 两端对齐, 缩进: 首行缩进: 2 字符, 行距: 1.5 倍  
行距

461 past three decades, 188 GLOF events have been recorded in the HMA (Shrestha et al., 2023), of which  
462 55 events (29%) occurred in glacier-proglacial lake systems. The main triggers of these floods include  
463 ice avalanches (Sherpa et al., 2025) and slope instability caused by rapid glacier retreat, leading to  
464 landslides into the lakes (Zheng et al., 2021a). Due to the continuous impact of climate warming, the  
465 interactions between glaciers and proglacial lakes may become increasingly complex in the coming  
466 decades. The number and size of glacial lakes may further increase, and the relationships between  
467 glaciers and proglacial lakes may undergo significant changes. As a result, traditional climate-based  
468 disaster risk models may not fully capture these complex, nonlinear interactions, especially those  
469 involving glacial lake expansion and glacier retreat. To effectively address these challenges, future  
470 disaster risk management strategies must be more comprehensive and forward-looking. This should  
471 include strengthening monitoring and early warning systems for GLOFs, incorporating the evolution of  
472 glacier-lake contact relationships, and considering glacier morphological characteristics to improve  
473 prediction capabilities.

设置了格式: 字体: (默认) Times New Roman, 10 磅

## 474 **6 Conclusions**

475 Using Landsat imagery, we applied a semi-automated mapping approach in Google Earth Engine  
476 (GEE) to inventory proglacial lakes across High Mountain Asia (HMA) in the 1990s and 2020s, and  
477 compiled the first region-wide dataset of LTGs and their proglacial lakes. In 2022, HMA contained 1740  
478 LTGs ( $5082.08 \pm 13.15 \text{ km}^2$ ), of which 667 glaciers ( $3454.59 \pm 12.43 \text{ km}^2$ ) maintained lake contact  
479 since 1990, and 1073 glaciers ( $1,627.49 \pm 4.30 \text{ km}^2$ ) developed new proglacial lakes. These glaciers  
480 were mainly distributed between 2735 and 8016 m a.s.l. Additionally, 468 glaciers ( $960.13 \pm 3.18 \text{ km}$   
481  $^2$ ) lost lake contact during the period.

482 A total of 1768 proglacial lakes ( $262.10 \pm 0.89 \text{ km}^2$ ) were connected to glaciers in 2022, including  
483 645 lakes ( $207.18 \pm 0.82 \text{ km}^2$ ) with continuous glacier contact and 1123 newly formed lakes ( $54.85 \pm$   
484  $0.35 \text{ km}^2$ ). Lakes were mainly distributed between 2684 and 6012 m a.s.l. Meanwhile, 485 lakes ( $45.31$   
485  $\pm 0.34 \text{ km}^2$ ) lost glacier contact, with 25 disappearing entirely. From 1990 to 2022, LTGs retreated by  
486  $324.43 \pm 19.23 \text{ km}^2$  (-5.1%), while proglacial lake area increased by  $138.19 \pm 1.18 \text{ km}^2$  (+81.7%).  
487 The development and evolution of lake-terminating glacier-proglacial lake systems are predominantly

488 concentrated along the southern margin of HMA, including the Hindu Kush, Himalayas,  
489 Nyainqentanglha, and Gangdise Mountains.

490 This dataset offers a robust basis for examining spatially heterogeneous glacier responses to climate  
491 change, coupled glacier–lake evolution, glacier hydrological modeling, glacial lake outburst flood  
492 (GLOF) assessment, and water resource management. Nevertheless, further improvements in data quality  
493 remain necessary, particularly in quantifying glacier–lake contact line length, the degree of glacier–lake  
494 contact (e.g., lake depth and subaqueous glacier front depth), and water temperature measurements.

495

496 **Financial support.** This work was funded by the National Key R&D Program of China (Grant No.  
497 2024YFC3013400) and National Science Foundation of China (Grant No. 42361144874).

498

499 **Author contributions.** YL designed the study, developed the methodology, performed analysis, and  
500 wrote the manuscript. QL provided funding, support and supervision. XL, YY and JY produced data and  
501 performed analysis. All other authors discussed and drafted the formulation of the specifications of the  
502 glacial lake inventory in this study. All authors contributed to the final form of the paper.

503 **Competing interests.** The authors declare that they have no conflict of interest.

504

505 **Code and data availability.** Data described in this manuscript can be accessed at Zenodo under  
506 <https://doi.org/10.5281/zenodo.17369580> (Luo and Liu, 2025). The code for proglacial lake ident  
507 -ification ~~is included in the supplementary materials, can be accessed via [https://code.earthengin](https://code.earthengin</a></del><br/>508 <del><a href=)~~

509

510

Appendix A

**Table A-1 Glacier type statistics (number and area) across subregions**

Region	Glacier number				Glacier area (km <sup>2</sup> )							
					1990s				2020s			
	Type-1	Type-2	Type-3	Total	Type-1	Type-2	Type-3	Total	Type-1	Type-2	Type-3	Total
Central Himalaya	94	138	84	316	589.97±2.81	264.92±1.64	219.8±1.17	1074.7±3.46	552.77±2.71	244.8±1.56	202.67±1.11	1000.25±3.32
Western Himalaya	66	106	28	200	198.31±2.11	176.41±1.67	42.54±0.47	417.26±2.74	192.5±2.08	167.24±1.64	40.28±0.45	400.02±2.69
Eastern Himalaya	64	68	48	180	419.67±2.06	155.37±1.07	87.2±0.68	662.24±2.42	392.93±1.97	136.97±0.98	78.65±0.63	608.55±2.29
Gangdise Mountains	64	77	50	191	35.19±0.32	45.65±0.37	33.34±0.33	114.17±0.59	31.79±0.31	40.11±0.34	29.53±0.31	101.44±0.55
Hindu-Kush	61	75	12	148	26.49±0.31	45.82±0.41	8.71±0.17	81.02±0.54	23.58±0.29	41.34±0.39	7.83±0.16	72.74±0.51
Nyainqentanglhe	55	126	48	229	677.08±3.76	368.21±2.96	164.46±1.28	1209.75±4.95	650.54±3.73	350.51±2.91	154.73±1.22	1155.78±4.89
Altun-Shan/Eastern Kunlun-Shan	32	30	3	65	197.95±0.85	62.54±0.42	4.09±0.09	264.59±0.95	194.08±0.84	59.98±0.41	3.95±0.09	258.02±0.93
Northern-Western Tien-Shan	32	73	40	145	31.78±0.37	63.81±0.53	37.44±0.35	133.03±0.74	28.79±0.35	58.39±0.51	33.45±0.33	120.63±0.7
Western Pamir	30	59	17	106	93.74±0.95	99.99±0.84	16.58±0.29	210.3±1.09	89.95±0.93	94.04±0.8	15.33±0.28	199.33±1.26
Central Tien-Shan	25	49	17	91	733.67±10.9	53.48±0.64	29.86±0.6	817.01±10.94	729.83±10.9	49.1±0.61	27.78±0.57	806.71±10.93
Qilian-Shan	21	7	10	38	119.22±0.92	11.38±0.19	59.35±0.54	189.95±1.08	116.6±0.9	10.31±0.18	57.66±0.52	184.57±1.05
Eastern Tien-Shan	18	46	18	82	33.23±0.54	39.06±0.38	29.91±0.54	102.2±0.85	30.49±0.52	35.32±0.36	27.46±0.52	93.27±0.82
Karakorum	18	18	6	42	66.51±0.78	102.9±0.99	128.82±2.25	298.24±2.58	65.1±0.76	100.62±0.97	128.1±2.25	293.82±2.56
Tanggula-Shan	17	17	27	61	130.26±0.94	14.97±0.24	62.7±0.54	207.93±1.11	124.33±0.91	13.75±0.23	58.63±0.52	196.7±1.07
Tibetan Interior Mountains	17	34	9	60	96.32±0.72	112.16±0.74	53.53±0.49	262.02±1.14	95.32±0.71	109.47±0.73	51.62±0.46	256.4±1.12
Dzhungarsky Alatau	16	45	14	75	12.85±0.2	32.15±0.31	17.71±0.26	62.71±0.45	10.78±0.18	28.49±0.29	15.41±0.24	54.68±0.42
Hengduan-Shan	16	65	27	108	10.75±0.18	49.63±0.5	27.82±0.31	88.2±0.61	8.03±0.16	42.71±0.47	22.99±0.27	73.73±0.57
Pamir-Alay	11	29	8	48	5.79±0.12	27.8±0.38	3.42±0.11	37±0.42	5.12±0.12	25.74±0.37	3.05±0.11	33.91±0.4
Western Kunlun-Shan	7	0	0	7	104.03±1.08	0	0	104.03±1.08	103.14±1.08	0	0	103.14±1.08
Eastern Pamir	2	5	1	8	6.89±0.22	14.14±0.28	0.39±0.03	21.43±0.35	6.82±0.21	13.78±0.27	0.37±0.03	20.97±0.35
Eastern Tibetan Mountains	1	6	1	8	2.35±0.08	5.75±0.14	0.76±0.05	8.86±0.16	2.12±0.08	4.83±0.14	0.64±0.04	7.59±0.16
<b>Total</b>	<b>667</b>	<b>1073</b>	<b>468</b>	<b>2208</b>	<b>3592.05±12.49</b>	<b>1746.17±4.43</b>	<b>1028.43±3.28</b>	<b>6366.64±13.65</b>	<b>3454.59±12.43</b>	<b>1627.49±4.3</b>	<b>960.13±3.18</b>	<b>6042.24±13.53</b>

设置了格式: 英语(美国)

**Table A 2 Area and number distribution of three glacier types across different size classes**

Glacier size (km <sup>2</sup> )	Glacier number (1990s)				Glacier number (2022s)				Glacier area (km <sup>2</sup> )(1990s)				Glacier area (km <sup>2</sup> )(2022s)			
	Type 1	Type 2	Type 3	Total	Type 1	Type 2	Type 3	Total	Type 1	Type 2	Type 3	Total	Type 1	Type 2	Type 3	Total
<0.05	8	9	4	21	20	33	19	72	0.31±0.03	0.33±0.03	0.15±0.02	0.78±0.04	0.72±0.04	1.05±0.05	0.69±0.04	2.46±0.07
0.05-0.1	28	43	26	97	37	72	28	137	2.22±0.07	3.24±0.08	1.86±0.06	7.32±0.12	2.72±0.08	5.36±0.11	2.07±0.06	10.15±0.15
0.1-0.5	166	437	136	739	168	442	151	761	44.18±0.34	118.86±0.54	39.44±0.31	202.48±0.71	45.06±0.34	118.54±0.54	43.13±0.33	206.73±0.72
0.5-1	126	239	101	466	118	205	86	409	92.8±0.53	166.86±0.72	71.75±0.47	331.41±1.01	84.4±0.52	141.21±0.66	60.88±0.44	286.49±0.94
1-5	192	272	154	628	188	256	141	585	478.95±1.49	563.75±1.61	343.68±1.24	1386.38±2.52	459.59±1.47	515.28±1.55	318.5±1.18	1289.21±2.44
5-10	71	43	30	144	67	41	26	134	498.24±1.92	303.8±1.57	207.84±1.19	1009.87±2.75	455.09±1.82	287.6±1.51	180.33±1.09	927.97±2.56
10-50	63	23	16	102	61	22	16	99	1347.15±4.57	432.18±2.45	248.78±1.6	2028.11±5.43	1268.56±4.37	432.17±2.49	240.09±1.54	1931.43±5.26
50-100	5	2	0	7	5	2	0	7	342.42±2.96	157.16±2.78	0	500.58±4.06	332.14±2.97	155.79±2.76	0	487.93±4.05
>100	3	0	1	4	3	0	1	4	784.78±10.96	0	114.93±2.23	899.7±11.18	785.42±10.96	0	114.44±2.23	899.86±11.18
Total	667	1073	468	2208	667	1073	468	2208	3592.05±12.49	1746.17±4.43	1028.43±3.28	6366.64±13.65	3454.59±12.43	1627.49±4.3	960.13±3.18	6042.24±13.53

**Table A.3 Glacial lake type statistics (number and area) across subregions**

Region	Lake number (1990s)				Lake number (2022s)				Lake area (km <sup>2</sup> ) (1990s)				Lake area (km <sup>2</sup> ) (2022s)			
	Type-1	Type-2	Type-3	Total	Type-1	Type-2	Type-3	Total	Type-1	Type-2	Type-3	Total	Type-1	Type-2	Type-3	Total
Central-Himalaya	91	0	86	177	91	149	80	320	46.47±0.38	0	13.83±0.2	60.29±0.43	76.89±0.51	10.02±0.16	15.7±0.21	102.62±0.58
Western-Himalaya	65	0	28	93	65	107	27	199	4.17±0.11	0	1.2±0.05	5.38±0.12	9.02±0.15	4.13±0.09	1.51±0.06	14.66±0.19
Eastern-Himalaya	57	0	50	107	56	75	49	180	23.92±0.26	0	5.05±0.11	28.98±0.29	36.75±0.36	10.89±0.18	6.55±0.13	54.19±0.42
Gangdise-Mountains	65	0	51	116	65	79	51	195	3.72±0.1	0	3.19±0.08	6.91±0.13	4.49±0.1	2.32±0.07	2.67±0.07	9.48±0.14
Hindu-Kush	60	0	12	72	61	75	12	148	2.97±0.08	0	0.61±0.04	3.58±0.09	4.83±0.11	1.81±0.06	0.49±0.04	7.13±0.12
Nyainqentanglha	52	0	51	103	52	135	49	236	12.53±0.18	0	5.78±0.13	18.31±0.22	28.57±0.3	8.16±0.14	7.52±0.14	44.25±0.36
Altun-Shan/Eastern-Kunlun-Shan	33	0	3	36	32	38	3	73	4.83±0.14	0	0.17±0.02	5±0.14	5.68±0.14	1.06±0.05	0.11±0.02	6.85±0.15
Northern/Western-Tien-Shan	32	0	41	73	31	75	39	145	1.15±0.05	0	1.44±0.05	2.6±0.07	2.3±0.07	1.97±0.06	1.51±0.06	5.77±0.11
Western-Pamir	28	0	19	47	28	60	19	107	1.27±0.05	0	0.91±0.04	2.17±0.07	2.81±0.08	3.04±0.08	0.89±0.04	6.74±0.12
Central-Tien-Shan	26	0	17	43	25	49	16	90	10.78±0.17	0	0.71±0.04	11.49±0.18	10.37±0.21	1.81±0.06	0.81±0.04	13±0.22
Qilian-Shan	20	0	11	31	20	8	11	39	2.81±0.07	0	0.95±0.04	3.76±0.09	4.24±0.1	0.26±0.02	0.88±0.04	5.37±0.11
Eastern-Tien-Shan	17	0	20	37	17	47	16	80	0.76±0.04	0	0.73±0.04	1.49±0.05	1.72±0.06	1.56±0.05	0.8±0.04	4.08±0.09
Karakoram	19	0	5	24	19	17	3	39	1.69±0.07	0	0.32±0.03	2.02±0.07	2.64±0.08	0.98±0.04	0.05±0.01	3.66±0.09
Tanggula-Shan	17	0	28	45	17	17	26	60	3.1±0.08	0	2.28±0.09	5.38±0.12	6.15±0.12	0.57±0.03	1.35±0.05	8.07±0.14
Tibetan-Interior-Mountains	14	0	9	23	14	35	7	56	2.56±0.11	0	0.94±0.05	3.5±0.12	3.58±0.14	1.75±0.06	0.91±0.04	6.23±0.16
Dzhungarsky-Alatau	14	0	16	30	14	48	15	77	0.37±0.03	0	1.17±0.05	1.54±0.06	1.03±0.05	1.38±0.05	1.25±0.05	3.66±0.09
Hengduan-Shan	15	0	28	43	15	66	27	108	0.71±0.04	0	1.63±0.06	2.35±0.07	1.26±0.06	1.84±0.06	1.91±0.07	5.01±0.11
Pamir-Alay	12	0	8	20	12	32	8	52	0.5±0.03	0	0.34±0.02	0.84±0.02	0.77±0.04	0.94±0.04	0.33±0.02	2.03±0.05
Western-Kunlun-Shan	7	0	0	7	7	0	0	7	3.17±0.08	0	0	3.17±0.08	3.59±0.09	0	0	3.59±0.09
Eastern-Pamir	3	0	1	4	3	5	1	9	0.22±0.03	0	0.05±0.01	0.26±0.03	0.33±0.02	0.16±0.02	0.04±0.01	0.53±0.03
Eastern-Tibetan-Mountains	1	0	1	2	1	6	1	8	0.1±0.01	0	0.04±0.01	0.14±0.02	0.19±0.02	0.21±0.02	0.02±0.01	0.42±0.03
Total	648	0	485	1133	645	1123	460	2228	127.82±0.61	0	41.33±0.32	169.15±0.69	207.18±0.82	54.85±0.35	45.31±0.34	307.34±0.96

**Table A 4 Area and number distribution of three lake types across different size classes**

Glacier size (km <sup>2</sup> )	Lake number								Lake area (km <sup>2</sup> )							
	1990s				2022s				1990s				2022s			
	Type 1	Type 2	Type 3	Total	Type 1	Type 2	Type 3	Total	Type 1	Type 2	Type 3	Total	Type 1	Type 2	Type 3	Total
<0.05	338	0	289	627	197	887	245	1329	7.62±0.12	0	7.5±0.12	15.12±0.16	5.71±0.11	20.58±0.19	6.13±0.11	32.42±0.25
0.05-0.1	96	0	93	189	145	155	92	392	6.58±0.12	0	6.45±0.12	13.03±0.17	10.02±0.15	10.81±0.15	6.56±0.12	27.39±0.24
0.1-0.5	157	0	90	247	204	72	111	387	32.46±0.28	0	17.77±0.21	50.24±0.34	47.07±0.35	13.19±0.17	23.25±0.24	83.51±0.46
0.5-1	30	0	12	42	47	6	9	62	20.03±0.25	0	8.44±0.17	28.47±0.3	31.18±0.32	4.43±0.14	5.67±0.13	41.28±0.37
≥1	27	0	1	28	52	3	3	58	61.12±0.45	0	1.17±0.06	62.29±0.45	113.19±0.65	5.84±0.12	3.7±0.12	122.73±0.67
<b>Total</b>	<b>648</b>	<b>0</b>	<b>485</b>	<b>1133</b>	<b>645</b>	<b>1123</b>	<b>460</b>	<b>2228</b>	<b>127.82±0.61</b>	<b>0</b>	<b>41.33±0.32</b>	<b>169.15±0.69</b>	<b>207.18±0.82</b>	<b>54.85±0.35</b>	<b>45.31±0.34</b>	<b>307.34±0.96</b>

**Table A.5 Area changes of different glacier types in each subregion (1990–2022)**

Region	Area loss(km <sup>2</sup> )				Area loss(%)			
	Type 1	Type 2	Type 3	Total	Type 1	Type 2	Type 3	Total
Central Himalaya	37.2±3.91	20.13±2.26	17.13±1.62	74.46±4.8	6.31	7.6	7.79	6.93
Western Himalaya	5.81±2.97	9.17±2.24	2.26±0.65	17.24±3.84	2.93	5.2	5.31	4.13
Eastern Himalaya	26.74±2.85	18.41±1.45	8.55±0.93	53.7±3.23	6.37	11.85	9.8	8.11
Gangdise Mountains	3.39±0.44	5.54±0.5	3.8±0.46	12.73±0.81	9.65	12.14	11.41	11.16
Hindu Kush	2.91±0.43	4.48±0.56	0.88±0.23	8.27±0.74	10.98	9.78	10.13	10.21
Nyainqentangha	26.54±5.29	17.7±4.15	9.72±1.77	53.96±6.95	3.92	4.81	5.91	4.46
Altun Shan/Eastern Kunlun Shan	3.87±1.19	2.57±0.59	0.14±0.13	6.58±1.33	1.95	4.1	3.38	2.48
Northern/Western Tien Shan	2.99±0.51	5.42±0.74	3.99±0.49	12.4±1.02	9.42	8.49	10.66	9.32
Western Pamir	3.79±1.33	5.95±1.16	1.24±0.4	10.98±1.81	4.04	5.95	7.51	5.22
Central Tien Shan	3.84±15.42	4.38±0.88	2.08±0.83	10.3±15.47	0.52	8.19	6.97	1.26
Qilian Shan	2.62±1.28	1.07±0.27	1.7±0.75	5.39±1.51	2.2	9.4	2.86	2.84
Eastern Tien Shan	2.74±0.75	2.74±0.52	2.45±0.75	8.93±1.18	8.25	9.58	8.18	8.74
Karakoram	1.41±1.09	2.29±1.39	0.72±3.18	4.42±3.64	2.12	2.22	0.56	1.48
Tanggula Shan	5.94±1.31	1.22±0.33	4.07±0.75	11.23±1.55	4.56	8.18	6.49	5.4
Tibetan Interior Mountains	1.01±1.02	2.69±1.04	1.92±0.68	5.62±1.61	1.04	2.4	3.58	2.14
Dzhungarsky Alatau	2.07±0.26	3.66±0.43	2.3±0.36	8.03±0.62	16.1	11.38	12.99	12.8
Hengduan Shan	2.73±0.24	6.92±0.69	4.83±0.41	14.48±0.84	25.34	13.95	17.37	16.42
Pamir Alay	0.67±0.17	2.06±0.53	0.37±0.15	3.1±0.58	11.55	7.4	10.75	8.36
Western Kunlun Shan	0.89±1.53	0	0	0.89±1.53	0.86	0	0	0.86
Eastern Pamir	0.08±0.3	0.36±0.39	0.02±0.04	0.46±0.49	1.1	2.57	5.37	2.15
Eastern Tibetan Mountains	0.23±0.11	0.92±0.19	0.12±0.06	1.27±0.23	9.81	15.94	16.33	14.35
Total	137.46±17.62	118.68±6.18	68.29±4.58	324.43±19.23	3.83	6.8	6.64	5.1

设置了格式: 英语(美国)

**Table A.6 Area and number changes of three glacier types across different size classes**

Glacier size- (km <sup>2</sup> )	Number change(count)				Area change(km <sup>2</sup> )				Area change(%)			
	Type-1	Type-2	Type-3	Total	Type-1	Type-2	Type-3	Total	Type-1	Type-2	Type-3	Total
<0.05	12	24	15	51	0.41±0.05	0.73±0.05	0.54±0.04	1.68±0.08	133.95	224.58	367.1	215.87
0.05-0.1	9	29	2	40	0.58±0.1	2.04±0.13	0.21±0.09	2.83±0.19	26.17	62.92	11.3	38.68
0.1-0.5	2	5	15	22	1.67±0.48	-1.1±0.77	3.68±0.46	4.25±1.02	3.78	-0.93	9.33	2.1
0.5-1	-8	-34	-15	-57	-8.41±0.74	-25.65±0.97	-10.87±0.64	-44.93±1.38	-9.06	-15.37	-15.15	-13.56
1-5	-9	-21	-13	-43	-19.48±2.14	-52.52±2.21	-25.17±1.71	-97.17±3.5	-4.07	-9.32	-7.32	-7.04
5-10	-4	-2	-4	-10	-38.2±2.62	-16.19±2.18	-27.51±1.57	-81.9±3.75	-7.67	-5.33	-13.24	-8.14
10-50	-2	-1	0	-3	-62.39±6.38	-24.61±3.4	-8.69±2.22	-96.69±7.56	-4.71	-5.69	-3.49	-4.77
50-100	0	0	0	0	-11.28±4.19	-1.37±3.92	0	-12.65±5.74	-3.28	-0.87		-2.53
>100	0	0	0	0	0.64±15.5	0	-0.48±3.15	0.16±15.82	0.08		-0.42	0.02
Total	0	0	0	0	-137.46±17.62	-118.67±6.17	-68.29±4.57	-324.42±27.18	-3.83	-6.8	-6.64	-5.1

**Table A.7 Area changes of different glacial lake types in each subregion (1990–2022)**

Region	Area change (km <sup>2</sup> )				Area change (%)		
	Type-1	Type-2	Type-3	Total	Type-1	Type-3	Total
Central Himalaya	30.42±0.64	10.02±0.16	1.88±0.29	42.32±0.73	65.46	13.6	79.19
Western Himalaya	4.84±0.19	4.13±0.09	0.21±0.07	9.28±0.22	115.95	25.8	172.62
Eastern Himalaya	12.82±0.45	10.89±0.18	1.49±0.17	25.22±0.51	53.63	29.49	87.04
Gangdise Mountains	0.77±0.14	2.32±0.07	-0.52±0.11	2.57±0.19	20.7	-16.32	37.21
Hindu-Kush	1.86±0.13	1.81±0.06	-0.11±0.05	3.55±0.15	62.57	-18.1	99.15
Nyainqentanglha	16.04±0.35	8.16±0.14	1.74±0.19	25.95±0.42	128.03	30.11	141.75
Altun-Shan/Eastern Kunlun-Shan	0.85±0.2	1.06±0.05	-0.05±0.02	1.86±0.21	17.59	-30.3	37.21
Northern/Western-Tien-Shan	1.14±0.09	1.97±0.06	0.07±0.08	3.17±0.13	98.76	4.86	122.14
Western Pamir	1.54±0.09	3.04±0.08	-0.02±0.06	4.57±0.14	121.66	-2.2	210.24
Central-Tien-Shan	-0.41±0.27	1.81±0.06	0.11±0.06	1.51±0.28	-3.8	15.59	13.14
Qilian-Shan	1.43±0.12	0.26±0.02	-0.07±0.06	1.61±0.14	50.93	-7.34	42.8
Eastern-Tien-Shan	0.96±0.08	1.56±0.05	0.07±0.06	2.59±0.11	126.23	9.62	174
Karakoram	0.94±0.11	0.98±0.04	-0.28±0.03	1.64±0.12	55.52	-86.41	81.3
Tungguin-Shan	3.04±0.14	0.57±0.03	-0.93±0.1	2.69±0.18	98.01	-40.83	59
Tibetan Interior Mountains	1.02±0.18	1.75±0.06	-0.03±0.07	2.73±0.2	39.92	-3.18	78.03
Dzhungursky Alatau	0.66±0.06	1.38±0.05	0.08±0.07	2.12±0.1	176.38	6.85	137.53
Hengduan Shan	0.55±0.07	1.84±0.06	0.28±0.09	2.66±0.13	76.97	17.13	113.23
Pamir-Alay	0.27±0.05	0.94±0.04	-0.02±0.03	1.19±0.07	54.26	-5.82	141.49
Western-Kunlun-Shan	0.42±0.12	0	0	0.42±0.12	13.26		13.26
Eastern Pamir	0.11±0.04	0.16±0.02	-0.01±0.01	0.26±0.04	50.87	-20.66	98.25
Eastern Tibetan Mountains	0.08±0.02	0.21±0.02	-0.01±0.01	0.28±0.04	77.14	-27.51	199.92
<b>Total</b>	<b>79.36±1.02</b>	<b>54.85±0.35</b>	<b>3.98±0.47</b>	<b>138.19±1.18</b>	<b>62.09</b>	<b>9.63</b>	<b>81.7</b>

**Table A.8 Area and number changes of proglacial lakes of three glacier types across different size classes**

Glacier size (km <sup>2</sup> )	Number change				Area change (km <sup>2</sup> )				Area change (%)		
	Type-1	Type-2	Type-3	Total	Type-1	Type-2	Type-3	Total	Type-1	Type-3	Total
<0.05	-141	887	-44	702	-1.91±0.16	20.58±0.19	-1.36±0.16	17.31±0.3	-25.07	-18.14	114.49
0.05-0.1	49	155	-1	203	3.44±0.19	10.81±0.15	0.11±0.17	14.36±0.29	52.27	1.71	110.23
0.1-0.5	47	72	21	140	14.61±0.44	13.19±0.17	5.47±0.32	33.27±0.57	45	30.77	66.22
0.5-1	17	6	-3	20	11.15±0.4	4.43±0.14	-2.76±0.21	12.82±0.48	55.66	-32.73	45.04
>1	25	3	2	30	52.07±0.79	5.84±0.12	2.53±0.13	60.44±0.81	85.19	215.49	97.02
<b>Total</b>	<b>-3</b>	<b>1123</b>	<b>-25</b>	<b>1095</b>	<b>79.36±1.02</b>	<b>54.85±0.35</b>	<b>3.98±0.46</b>	<b>138.19±1.18</b>	<b>62.09</b>	<b>9.63</b>	<b>81.7</b>

设置了格式: 英语(美国)

## Reference

- [Benn, D. I., Hulton, N. R. J., and Mottram, R. H.: 'Calving laws', 'sliding laws' and the stability of tidewater glaciers, \*Ann Glaciol\*, 46, 123-130, 10.3189/172756407782871161, 2007a.](#)
- [Benn, D. I., Warren, C. R., and Mottram, R. H.: Calving processes and the dynamics of calving glaciers, \*Earth-Science Reviews\*, 82, 143-179, 10.1016/j.earscirev.2007.02.002, 2007b.](#)
- [Bolch, T., Menounos, B., and Wheate, R.: Landsat-based inventory of glaciers in western Canada, 1985–2005, \*Remote Sens Environ\*, 114, 127-137, <https://doi.org/10.1016/j.rse.2009.08.015>, 2010.](#)
- [Brun, F., Berthier, E., Wagnon, P., Kaab, A., and Treichler, D.: A spatially resolved estimate of High Mountain Asia glacier mass balances, 2000-2016, \*Nat Geosci\*, 10, 668-673, 10.1038/NGEO2999, 2017.](#)
- [Brun, F., Wagnon, P., Berthier, E., Jomelli, V., Maharjan, S. B., Shrestha, F., and Kraaijenbrink, P. D. A.: Heterogeneous Influence of Glacier Morphology on the Mass Balance Variability in High Mountain Asia, \*Journal of Geophysical Research: Earth Surface\*, 124, 1331-1345, 10.1029/2018jf004838, 2019.](#)
- [Carrivick, J. L. and Tweed, F. S.: Proglacial lakes: character, behaviour and geological importance, \*Quaternary Sci Rev\*, 78, 34-52, 10.1016/j.quascirev.2013.07.028, 2013.](#)
- [Chen, F., Zhang, M., Guo, H., Allen, S., Kargel, J. S., Haritashya, U. K., and Watson, C. S.: Annual 30 m dataset for glacial lakes in High Mountain Asia from 2008 to 2017, \*Earth System Science Data\*, 13, 741-766, 10.5194/essd-13-741-2021, 2021.](#)
- [Chernos, M., Koppes, M., and Moore, R. D.: Ablation from calving and surface melt at lake-terminating Bridge Glacier, British Columbia, 1984–2013, \*The Cryosphere\*, 10, 87-102, 10.5194/tc-10-87-2016, 2016.](#)
- [Foga, S., Scaramuzza, P. L., Guo, S., Zhu, Z., Dilley, R. D., Beckmann, T., Schmidt, G. L., Dwyer, J. L., Joseph Hughes, M., and Laue, B.: Cloud detection algorithm comparison and validation for operational Landsat data products, \*Remote Sens Environ\*, 194, 379-390, <https://doi.org/10.1016/j.rse.2017.03.026>, 2017.](#)
- [Gardelle, J., Berthier, E., and Arnaud, Y.: Slight mass gain of Karakoram glaciers in the early twenty-first century, \*Nat Geosci\*, 5, 322-325, 10.1038/Ngeo1450, 2012.](#)
- [Hanshaw, M. N. and Bookhagen, B.: Glacial areas, lake areas, and snow lines from 1975 to 2012: status of the Cordillera Vilcanota, including the Queleccaya Ice Cap, northern central Andes, Peru, \*The\*](#)

[Cryosphere, 8, 359-376, 10.5194/tc-8-359-2014, 2014.](#)

[Hugonnet, R., McNabb, R., Berthier, E., Menounos, B., Nuth, C., Girod, L., Farinotti, D., Huss, M., Dussailant, I., Brun, F., and Kaab, A.: Accelerated global glacier mass loss in the early twenty-first century. \*Nature\*, 592, 726-731, 10.1038/s41586-021-03436-z, 2021.](#)

[Kääb, A., Treichler, D., Nuth, C., and Berthier, E.: Brief Communication: Contending estimates of 2003–2008 glacier mass balance over the Pamir–Karakoram–Himalaya. \*The Cryosphere\*, 9, 557-564, 10.5194/tc-9-557-2015, 2015.](#)

[Khanal, S., Tiwari, S., Lutz, A. F., Hurk, B. V. D., and Immerzeel, W. W.: Historical Climate Trends over High Mountain Asia Derived from ERA5 Reanalysis Data. \*Journal of Applied Meteorology and Climatology\*, 62, 263-288, <https://doi.org/10.1175/JAMC-D-21-0045.1>, 2023.](#)

[Li, D., Shangguan, D., and Anjum, M. N.: Glacial Lake Inventory Derived from Landsat 8 OLI in 2016–2018 in China–Pakistan Economic Corridor. \*ISPRS International Journal of Geo-Information\*, 9, 10.3390/ijgi9050294, 2020.](#)

[Li, J. and Sheng, Y.: An automated scheme for glacial lake dynamics mapping using Landsat imagery and digital elevation models: a case study in the Himalayas. \*Int J Remote Sens\*, 33, 5194-5213, 10.1080/01431161.2012.657370, 2012.](#)

[Liu, Q., Maver, C., Wang, X., Nie, Y., Wu, K., Wei, J., and Liu, S.: Interannual flow dynamics driven by frontal retreat of a lake-terminating glacier in the Chinese Central Himalaya. \*Earth Planet Sc Lett\*, 546, 10.1016/j.epsl.2020.116450, 2020.](#)

[Luo, W., Zhang, G., Chen, W., and Xu, F.: Response of glacial lakes to glacier and climate changes in the western Nyainqentanglha range. \*Sci Total Environ\*, 735, 139607, 10.1016/j.scitotenv.2020.139607, 2020.](#)

[Luo, Y. and Liu, Q.: Rapidly Changing Lake-Terminating Glaciers in High Mountain Asia: A Dataset from 1990 to 2022, Zenodo \[dataset\], <https://doi.org/10.5281/zenodo.17369580>, 2025.](#)

[Luo, Y., Yin, Y., Zhong, Y., Lu, X., Yang, J., Sapkota, L., Lu, X., and Liu, Q.: Dynamics of lake-terminating glaciers in the Himalaya and Southeastern Tibet between 1990 and 2020. \*Journal of Glaciology\*, 1-20, 10.1017/jog.2025.10088, 2025.](#)

[Maurer, J. M., Schaefer, J. M., Rupper, S., and Corley, A.: Acceleration of ice loss across the Himalayas over the past 40 years. \*Science Advances\*, 5, eaav7266, doi:10.1126/sciadv.aav7266, 2019.](#)

[Mertes, J. R., Thompson, S. S., Booth, A. D., Gullely, J. D., and Benn, D. I.: A conceptual model of supra-](#)

[glacial lake formation on debris-covered glaciers based on GPR facies analysis, Earth Surface Processes and Landforms](https://doi.org/10.1002/esp.4068), 42, 903-914, <https://doi.org/10.1002/esp.4068>, 2017.

[Minowa, M., Schaefer, M., and Skvarca, P.: Effects of topography on dynamics and mass loss of lake-terminating glaciers in southern Patagonia, Journal of Glaciology](https://doi.org/10.1017/jog.2023.42), 1-18, [10.1017/jog.2023.42](https://doi.org/10.1017/jog.2023.42), 2023.

[Pronk, J. B., Bolch, T., King, O., Wouters, B., and Benn, D. I.: Contrasting surface velocities between lake- and land-terminating glaciers in the Himalayan region, The Cryosphere](https://doi.org/10.5194/tc-15-5577-2021), 15, 5577-5599, [10.5194/tc-15-5577-2021](https://doi.org/10.5194/tc-15-5577-2021), 2021.

[Quincey, D. J., Richardson, S. D., Luckman, A., Lucas, R. M., Reynolds, J. M., Hambrey, M. J., and Glasser, N. F.: Early recognition of glacial lake hazards in the Himalaya using remote sensing datasets, Global Planet Change](https://doi.org/10.1016/j.gloplacha.2006.07.013), 56, 137-152, [10.1016/j.gloplacha.2006.07.013](https://doi.org/10.1016/j.gloplacha.2006.07.013), 2007.

[Salerno, F., Thakuri, S., D'Agata, C., Smiraglia, C., Manfredi, E. C., Viviano, G., and Tartari, G.: Glacial lake distribution in the Mount Everest region: Uncertainty of measurement and conditions of formation, Global Planet Change](https://doi.org/10.1016/j.gloplacha.2012.04.001), 92-93, 30-39, [10.1016/j.gloplacha.2012.04.001](https://doi.org/10.1016/j.gloplacha.2012.04.001), 2012.

[Sato, Y., Fujita, K., Inoue, H., and Sakai, A.: Land- to lake-terminating transition triggers dynamic thinning of a Bhutanese glacier, The Cryosphere](https://doi.org/10.5194/tc-16-2643-2022), 16, 2643-2654, [10.5194/tc-16-2643-2022](https://doi.org/10.5194/tc-16-2643-2022), 2022.

[Sherpa, S. F., Smith, L. C., Wang, B., and Stuurman, C.: Brief Communication: Multisource Remote Sensing Detects Growing Himalayan Glacial Lake Outburst Flood Hazards, EGU sphere](https://doi.org/10.5194/egusphere-2025-133), 2025, 1-9, [10.5194/egusphere-2025-133](https://doi.org/10.5194/egusphere-2025-133), 2025.

[Shrestha, F., Steiner, J. F., Shrestha, R., Dhungel, Y., Joshi, S. P., Inglis, S., Ashraf, A., Wali, S., Walizada, K. M., and Zhang, T.: A comprehensive and version-controlled database of glacial lake outburst floods in High Mountain Asia, Earth System Science Data](https://doi.org/10.5194/essd-15-3941-2023), 15, 3941-3961, [10.5194/essd-15-3941-2023](https://doi.org/10.5194/essd-15-3941-2023), 2023.

[Shugar, D. H., Burr, A., Haritashya, U. K., Kargel, J. S., Watson, C. S., Kennedy, M. C., Bevington, A. R., Betts, R. A., Harrison, S., and Strattman, K.: Rapid worldwide growth of glacial lakes since 1990, Nat Clim Change](https://doi.org/10.1038/s41558-020-0855-4), 10, 939-945, [10.1038/s41558-020-0855-4](https://doi.org/10.1038/s41558-020-0855-4), 2020.

[Steiner, J., Armstrong, W., Kochtitzky, W., McNabb, R., Aguayo, R., Bolch, T., Maussion, F., Agarwal, V., Barr, I., Baurley, N. R., Cloutier, M., DeWater, K., Donachie, F., Drocourt, Y., Garg, S., Joshi, G., Guzman, B., Kutuzov, S., Loriaux, T., Mathias, C., Menounos, B., Miles, E., Osika, A., Potter, K., Racoviteanu, A., Rick, B., Sterner, M., Tallentire, G. D., Tielidze, L., White, R., Wu, K., and Zheng, W.: Global mapping of lake-terminating glaciers, Earth Syst. Sci. Data Discuss.](https://doi.org/10.5194/essd-2025-315), 2025, 1-22, [10.5194/essd-2025-315](https://doi.org/10.5194/essd-2025-315), 2025.

[Sugiyama, S., Skvarca, P., Naito, N., Enomoto, H., Tsutaki, S., Tone, K., Marinsek, S., and Aniya, M.: Ice speed of a calving glacier modulated by small fluctuations in basal water pressure, \*Nat Geosci\*, 4, 597-600, 10.1038/ngeo1218, 2011.](#)

[Sutherland, J. L., Carrivick, J. L., Gandy, N., Shulmeister, J., Quincey, D. J., and Cornford, S. L.: Proglacial Lakes Control Glacier Geometry and Behavior During Recession, \*Geophysical Research Letters\*, 47, 10.1029/2020gl088865, 2020.](#)

[Truffer, M. and Motyka, R. J.: Where glaciers meet water: Subaqueous melt and its relevance to glaciers in various settings, \*Reviews of Geophysics\*, 54, 220-239, 10.1002/2015rg000494, 2016.](#)

[Tsutaki, S., Sugiyama, S., Nishimura, D., and Funk, M.: Acceleration and flotation of a glacier terminus during formation of a proglacial lake in Rhonegletscher, Switzerland, \*Journal of Glaciology\*, 59, 559-570, 10.3189/2013JoG12J107, 2017.](#)

[Tsutaki, S., Fujita, K., Nuimura, T., Sakai, A., Sugiyama, S., Komori, J., and Tshering, P.: Contrasting thinning patterns between lake- and land-terminating glaciers in the Bhutanese Himalaya, \*The Cryosphere\*, 13, 2733-2750, 10.5194/tc-13-2733-2019, 2019.](#)

[Wang, X., Guo, X., Yang, C., Liu, Q., Wei, J., Zhang, Y., Liu, S., Zhang, Y., Jiang, Z., and Tang, Z.: Glacial lake inventory of high-mountain Asia in 1990 and 2018 derived from Landsat images, \*Earth System Science Data\*, 12, 2169-2182, 10.5194/essd-12-2169-2020, 2020.](#)

[Worni, R., Huggel, C., and Stoffel, M.: Glacial lakes in the Indian Himalayas--from an area-wide glacial lake inventory to on-site and modeling based risk assessment of critical glacial lakes, \*Sci Total Environ\*, 468-469 Suppl, S71-84, 10.1016/j.scitotenv.2012.11.043, 2013.](#)

[Yao, T., Thompson, L., Yang, W., Yu, W., Gao, Y., Guo, X., Yang, X., Duan, K., Zhao, H., Xu, B., Pu, J., Lu, A., Xiang, Y., Kattel, D. B., and Joswiak, D.: Different glacier status with atmospheric circulations in Tibetan Plateau and surroundings, \*Nat Clim Change\*, 2, 663-667, 10.1038/nclimate1580, 2012.](#)

[Zhang, G., Yao, T., Xie, H., Wang, W., and Yang, W.: An inventory of glacial lakes in the Third Pole region and their changes in response to global warming, \*Global Planet Change\*, 131, 148-157, 10.1016/j.gloplacha.2015.05.013, 2015.](#)

[Zhang, G., Zheng, G., Gao, Y., Xiang, Y., Lei, Y., and Li, J.: Automated Water Classification in the Tibetan Plateau Using Chinese GF-1 WFV Data, \*Photogrammetric Engineering & Remote Sensing\*, 83, 509-519, 10.14358/pers.83.7.509, 2017.](#)

[Zhang, G., Bolch, T., Yao, T., Rounce, D. R., Chen, W., Voh, G., King, O., Allen, S. K., Wang, M., and](#)

Wang, W.: Underestimated mass loss from lake-terminating glaciers in the greater Himalaya, *Nat Geosci.*, 16, 333-338, 10.1038/s41561-023-01150-1, 2023.

Zheng, G., Mergili, M., Emmer, A., Allen, S., Bao, A., Guo, H., and Stoffel, M.: The 2020 glacial lake outburst flood at Jinwuco, Tibet: causes, impacts, and implications for hazard and risk assessment, *The Cryosphere*, 15, 3159-3180, 10.5194/tc-15-3159-2021, 2021a.

Zheng, G., Allen, S. K., Bao, A., Ballesteros-Cánovas, J. A., Huss, M., Zhang, G., Li, J., Yuan, Y., Jiang, L., Yu, T., Chen, W., and Stoffel, M.: Increasing risk of glacial lake outburst floods from future Third Pole deglaciation, *Nat Clim Change*, 11, 411-417, 10.1038/s41558-021-01028-3, 2021b.

Benn, D. I., Hulton, N. R. J., and Mottram, R. H.: 'Calving laws', 'sliding laws' and the stability of tidewater glaciers, *Ann Glaciol*, 46, 123-130, 10.3189/172756407782871161, 2007a.

Benn, D. I., Warren, C. R., and Mottram, R. H.: Calving processes and the dynamics of calving glaciers, *Earth Science Reviews*, 82, 143-179, 10.1016/j.earscirev.2007.02.002, 2007b.

Boleh, T., Menounos, B., and Wheate, R.: Landsat-based inventory of glaciers in western Canada, 1985-2005, *Remote Sens Environ*, 114, 127-137, <https://doi.org/10.1016/j.rse.2009.08.015>, 2010.

Brun, F., Berthier, E., Wagnon, P., Kaab, A., and Treichler, D.: A spatially resolved estimate of High Mountain Asia glacier mass balances, 2000-2016, *Nat Geosci.*, 10, 668-673, 10.1038/NGEO2999, 2017.

Brun, F., Wagnon, P., Berthier, E., Jomelli, V., Maharjan, S. B., Shrestha, F., and Kraaijenbrink, P. D. A.: Heterogeneous Influence of Glacier Morphology on the Mass Balance Variability in High Mountain Asia, *Journal of Geophysical Research: Earth Surface*, 124, 1331-1345, 10.1029/2018jf004838, 2019.

Carrivick, J. L. and Tweed, F. S.: Proglacial lakes: character, behaviour and geological importance, *Quaternary Sci Rev*, 78, 34-52, 10.1016/j.quascirev.2013.07.028, 2013.

Chen, F., Zhang, M., Guo, H., Allen, S., Kargel, J. S., Haritashya, U. K., and Watson, C. S.: Annual 30 m dataset for glacial lakes in High Mountain Asia from 2008 to 2017, *Earth System Science Data*, 13, 741-766, 10.5194/essd-13-741-2021, 2021.

Chernos, M., Koppes, M., and Moore, R. D.: Ablation from calving and surface melt at lake-terminating Bridge Glacier, British Columbia, 1984-2013, *The Cryosphere*, 10, 87-102, 10.5194/tc-10-87-2016, 2016.

Foga, S., Searamuzza, P. L., Guo, S., Zhu, Z., Dilley, R. D., Beekmann, T., Schmidt, G. L., Dwyer, J. L., Joseph Hughes, M., and Laue, B.: Cloud detection algorithm comparison and validation for operational

带格式的: 段落间距段后: 8 磅

Landsat data products, *Remote Sens Environ*, 194, 379–390, <https://doi.org/10.1016/j.rse.2017.03.026>, 2017.

Gardelle, J., Berthier, E., and Arnaud, Y.: Slight mass gain of Karakoram glaciers in the early twenty-first century, *Nat Geosci*, 5, 322–325, [10.1038/Ngeo1450](https://doi.org/10.1038/Ngeo1450), 2012.

Hanshaw, M. N. and Bookhagen, B.: Glacial areas, lake areas, and snow lines from 1975 to 2012: status of the Cordillera Vilcanota, including the Quelccaya Ice Cap, northern central Andes, Peru, *The Cryosphere*, 8, 359–376, [10.5194/tc-8-359-2014](https://doi.org/10.5194/tc-8-359-2014), 2014.

Hugonnet, R., McNabb, R., Berthier, E., Menounos, B., Nuth, C., Girod, L., Farinotti, D., Huss, M., Dussailant, I., Brun, F., and Kaab, A.: Accelerated global glacier mass loss in the early twenty-first century, *Nature*, 592, 726–731, [10.1038/s41586-021-03436-z](https://doi.org/10.1038/s41586-021-03436-z), 2021.

Kääb, A., Treichler, D., Nuth, C., and Berthier, E.: Brief Communication: Contending estimates of 2003–2008 glacier mass balance over the Pamir–Karakoram–Himalaya, *The Cryosphere*, 9, 557–564, [10.5194/tc-9-557-2015](https://doi.org/10.5194/tc-9-557-2015), 2015.

Li, D., Shangquan, D., and Anjum, M. N.: Glacial Lake Inventory Derived from Landsat 8 OLI in 2016–2018 in China–Pakistan Economic Corridor, *ISPRS International Journal of Geo-Information*, 9, [10.3390/ijgi9050294](https://doi.org/10.3390/ijgi9050294), 2020.

Li, J. and Sheng, Y.: An automated scheme for glacial lake dynamics mapping using Landsat imagery and digital elevation models: a case study in the Himalayas, *Int J Remote Sens*, 33, 5194–5213, [10.1080/01431161.2012.657370](https://doi.org/10.1080/01431161.2012.657370), 2012.

Liu, Q., Mayer, C., Wang, X., Nie, Y., Wu, K., Wei, J., and Liu, S.: Interannual flow dynamics driven by frontal retreat of a lake-terminating glacier in the Chinese Central Himalaya, *Earth Planet Sc Lett*, 546, [10.1016/j.epsl.2020.116450](https://doi.org/10.1016/j.epsl.2020.116450), 2020.

Luo, W., Zhang, G., Chen, W., and Xu, F.: Response of glacial lakes to glacier and climate changes in the western Nyainqentanglha range, *Sci Total Environ*, 735, 139607, [10.1016/j.scitotenv.2020.139607](https://doi.org/10.1016/j.scitotenv.2020.139607), 2020.

Luo, Y. and Liu, Q.: Rapidly Changing Lake Terminating Glaciers in High Mountain Asia: A Dataset from 1990 to 2022, Zenodo [dataset], <https://doi.org/10.5281/zenodo.17369580>, 2025.

Maurer, J. M., Schaefer, J. M., Rupper, S., and Corley, A.: Acceleration of ice loss across the Himalayas over the past 40 years, *Science Advances*, 5, eaav7266, [doi:10.1126/sciadv.aav7266](https://doi.org/10.1126/sciadv.aav7266), 2019.

Mertes, J. R., Thompson, S. S., Booth, A. D., Gullely, J. D., and Benn, D. I.: A conceptual model of supra-

glacial lake formation on debris-covered glaciers based on GPR facies analysis, *Earth Surface Processes and Landforms*, 42, 903–914, <https://doi.org/10.1002/esp.4068>, 2017.

Quincey, D. J., Richardson, S. D., Luckman, A., Lucas, R. M., Reynolds, J. M., Hambrey, M. J., and Glasser, N. F.: Early recognition of glacial lake hazards in the Himalaya using remote sensing datasets, *Global Planet Change*, 56, 137–152, [10.1016/j.gloplacha.2006.07.013](https://doi.org/10.1016/j.gloplacha.2006.07.013), 2007.

Salerno, F., Thakuri, S., D'Agata, C., Smiraglia, C., Manfredi, E. C., Viviano, G., and Tartari, G.: Glacial lake distribution in the Mount Everest region: Uncertainty of measurement and conditions of formation, *Global Planet Change*, 92–93, 30–39, [10.1016/j.gloplacha.2012.04.001](https://doi.org/10.1016/j.gloplacha.2012.04.001), 2012.

Sato, Y., Fujita, K., Inoue, H., and Sakai, A.: Land-to-lake-terminating transition triggers dynamic thinning of a Bhutanese glacier, *The Cryosphere*, 16, 2643–2654, [10.5194/te-16-2643-2022](https://doi.org/10.5194/te-16-2643-2022), 2022.

Shugar, D. H., Burr, A., Haritashya, U. K., Kargel, J. S., Watson, C. S., Kennedy, M. C., Bevington, A. R., Betts, R. A., Harrison, S., and Stratman, K.: Rapid worldwide growth of glacial lakes since 1990, *Nat Clim Change*, 10, 939–945, [10.1038/s41558-020-0855-4](https://doi.org/10.1038/s41558-020-0855-4), 2020.

Steiner, J., Armstrong, W., Koehntzky, W., McNabb, R., Aguayo, R., Bolch, T., Maussion, F., Agarwal, V., Barr, I., Baurley, N. R., Cloutier, M., DeWater, K., Donachie, F., Drocourt, Y., Garg, S., Joshi, G., Guzman, B., Kutuzov, S., Loriaux, T., Mathias, C., Menounos, B., Miles, E., Osika, A., Potter, K., Răeoviteanu, A., Riek, B., Sterner, M., Tallentire, G. D., Tielidze, L., White, R., Wu, K., and Zheng, W.: Global mapping of lake-terminating glaciers, *Earth Syst. Sci. Data Discuss.*, 2025, 1–22, [10.5194/essd-2025-315](https://doi.org/10.5194/essd-2025-315), 2025.

Sugiyama, S., Skvarea, P., Naito, N., Enomoto, H., Tsutaki, S., Tone, K., Marinsek, S., and Aniya, M.: Ice speed of a calving glacier modulated by small fluctuations in basal water pressure, *Nat Geosci*, 4, 597–600, [10.1038/ngeo1218](https://doi.org/10.1038/ngeo1218), 2011.

Sutherland, J. L., Carrivick, J. L., Gandy, N., Shulmeister, J., Quincey, D. J., and Cornford, S. L.: Proglacial Lakes Control Glacier Geometry and Behavior During Recession, *Geophysical Research Letters*, 47, [10.1029/2020gl088865](https://doi.org/10.1029/2020gl088865), 2020.

Truffer, M. and Motyka, R. J.: Where glaciers meet water: Subaqueous melt and its relevance to glaciers in various settings, *Reviews of Geophysics*, 54, 220–239, [10.1002/2015rg000494](https://doi.org/10.1002/2015rg000494), 2016.

Tsutaki, S., Sugiyama, S., Nishimura, D., and Funk, M.: Acceleration and flotation of a glacier terminus during formation of a proglacial lake in Rhonegletscher, Switzerland, *Journal of Glaciology*, 59, 559–570, [10.3189/2013Jog12J107](https://doi.org/10.3189/2013Jog12J107), 2017.

- Tsutaki, S., Fujita, K., Nuimura, T., Sakai, A., Sugiyama, S., Komori, J., and Tshering, P.: Contrasting thinning patterns between lake and land-terminating glaciers in the Bhutanese Himalaya, *The Cryosphere*, 13, 2733–2750, [10.5194/te-13-2733-2019](https://doi.org/10.5194/te-13-2733-2019), 2019.
- Wang, X., Guo, X., Yang, C., Liu, Q., Wei, J., Zhang, Y., Liu, S., Zhang, Y., Jiang, Z., and Tang, Z.: Glacial lake inventory of high-mountain Asia in 1990 and 2018 derived from Landsat images, *Earth System Science-Data*, 12, 2169–2182, [10.5194/essd-12-2169-2020](https://doi.org/10.5194/essd-12-2169-2020), 2020.
- Worni, R., Huggel, C., and Stoffel, M.: Glacial lakes in the Indian Himalayas – from an area-wide glacial lake inventory to on-site and modeling-based risk assessment of critical glacial lakes, *Sci Total Environ*, 468–469 Suppl, S71–84, [10.1016/j.scitotenv.2012.11.043](https://doi.org/10.1016/j.scitotenv.2012.11.043), 2013.
- Yao, T., Thompson, L., Yang, W., Yu, W., Gao, Y., Guo, X., Yang, X., Duan, K., Zhao, H., Xu, B., Pu, J., Lu, A., Xiang, Y., Kattel, D. B., and Joswiak, D.: Different glacier status with atmospheric circulations in Tibetan Plateau and surroundings, *Nat Clim Change*, 2, 663–667, [10.1038/nclimate1580](https://doi.org/10.1038/nclimate1580), 2012.
- Zhang, G., Yao, T., Xie, H., Wang, W., and Yang, W.: An inventory of glacial lakes in the Third Pole region and their changes in response to global warming, *Global Planet Change*, 131, 148–157, [10.1016/j.gloplacha.2015.05.013](https://doi.org/10.1016/j.gloplacha.2015.05.013), 2015.
- Zhang, G., Zheng, G., Gao, Y., Xiang, Y., Lei, Y., and Li, J.: Automated Water Classification in the Tibetan Plateau Using Chinese GF-1 WFV Data, *Photogrammetric Engineering & Remote Sensing*, 83, 509–519, [10.14358/pers.83.7.509](https://doi.org/10.14358/pers.83.7.509), 2017.
- Zhang, G., Bolch, T., Yao, T., Rounce, D. R., Chen, W., Voh, G., King, O., Allen, S. K., Wang, M., and Wang, W.: Underestimated mass loss from lake-terminating glaciers in the greater Himalaya, *Nat Geosci*, 16, 333–338, [10.1038/s41561-023-01150-1](https://doi.org/10.1038/s41561-023-01150-1), 2023.
- Zheng, G., Allen, S. K., Bao, A., Ballesteros-Cánovas, J. A., Huss, M., Zhang, G., Li, J., Yuan, Y., Jiang, L., Yu, T., Chen, W., and Stoffel, M.: Increasing risk of glacial lake outburst floods from future Third Pole deglaciation, *Nat Clim Change*, 11, 411–417, [10.1038/s41558-021-01028-3](https://doi.org/10.1038/s41558-021-01028-3), 2021.